Received: 7 February 2018 | Revised: 27 April 2018 | Accepted: 30 April 2018

DOI: 10.1002/cm.21449

RESEARCH ARTICLE

WILEY

The TOG protein Stu2/XMAP215 interacts covalently and noncovalently with SUMO

Matt Greenlee[1] | Annabel Alonso[1] | Maliha Rahman[1] | Nida Meednu[2] | Kayla Davis[1] | Victoria Tabb[1] | River Cook[1] | Rita K. Miller[1]

[1]Department of Biochemistry and Molecular Biology, Oklahoma State University, Stillwater, Oklahoma 74078

[2]Department of Biology, University of Rochester, Rochester, New York 14627

Correspondence
Rita K. Miller, 248A Noble Research Center, Department of Biochemistry and Molecular Biology, Oklahoma State University, Stillwater, Oklahoma 74078.
Email: rita.miller@okstate.edu

Funding information
Oklahoma Health Research Program of the Oklahoma Center for the Advancement of Science and Technology, Grant number: OCAST HR09-150S; NSF, Grant numbers: MCB-0414768, MCB-1052174; NIH, Grant number: R15GM119117-01; Oklahoma Agricultural Experiment Station, Grant number: OKL02961; Sloan Foundation; NSF-funded Louis Stokes Alliance for Minority Participation (OK-LSAMP) program at OSU

Correction added on Aug 14, 2019 after first online publication: The copyright line has been updated.

Abstract

Stu2p is the yeast member of the XMAP215/Dis1/ch-TOG family of microtubule-associated proteins that promote microtubule polymerization. However, the factors that regulate its activity are not clearly understood. Here we report that Stu2p in the budding yeast *Saccharomyces cerevisiae* interacts with SUMO by covalent and noncovalent mechanisms. Stu2p interacted by two-hybrid analysis with the yeast SUMO Smt3p, its E2 Ubc9p, and the E3 Nfi1p. A region of Stu2p containing the dimerization domain was both necessary and sufficient for interaction with SUMO and Ubc9p. Stu2p was found to be sumoylated both *in vitro* and *in vivo*. Stu2p copurified with SUMO in a pull-down assay and vice versa. Stu2p also bound to a nonconjugatable form of SUMO, suggesting that Stu2p can interact noncovalently with SUMO. In addition, Stu2p interacted with the STUbL enzyme Ris1p. Stu2p also copurified with ubiquitin in a pull-down assay, suggesting that it can be modified by both SUMO and ubiquitin. Tubulin, a major binding partner of Stu2p, also interacted noncovalently with SUMO. By two-hybrid analysis, the beta-tubulin Tub2p interacted with SUMO independently of the microtubule stressor, benomyl. Together, these findings raise the possibility that the microtubule polymerization activities mediated by Stu2p are regulated through sumoylation pathways.

KEYWORDS
microtubules, STU2, XMAP215, SUMO, tubulin, ubiquitin

1 | INTRODUCTION

Stu2p is the yeast member of the highly conserved XMAP215/Dis1/ch-TOG family of microtubule associated proteins (MAPs) that stimulate microtubule growth and block catastrophe (Al-Bassam, van Breugel, Harrison, & Hyman, 2006; Brouhard et al., 2008; Podolski, Mahamdeh, & Howard, 2014; Wang & Huffaker, 1997) (reviewed in Al-Bassam & Chang, 2011). The molecular basis of this property lies in the dual ability of Stu2p to bind free tubulin dimers and microtubule polymer. Binding to alpha-beta dimers occurs through its two TOG (Tumor Overexpressed Gene) domains (Al-Bassam, Larsen, Hyman, & Harrison, 2007; Al-Bassam et al., 2006; Ayaz, Ye, Huddleston, Brautigam, & Rice, 2012; Slep & Vale, 2007), and binding to the microtubule lattice occurs through its basic microtubule binding domain (Al-Bassam et al., 2006; Wang & Huffaker, 1997). Through a conformational change, Stu2p/ch-TOG facilitates the addition of dimers onto the plus end of the microtubule polymer (Al-Bassam et al., 2006). Although in most cases it has been seen to act as a microtubule polymerase (Podolski et al., 2014), in a few specific instances it has also been characterized as having a destabilizing effect (Al-Bassam & Chang, 2011; Al-Bassam et al., 2006; Brouhard et al., 2008; Humphrey, Felzer-Kim, & Joglekar, 2018; Shirasu-Hiza, Coughlin, & Mitchison, 2003; van Breugel, Drechsel, & Hyman, 2003).

Stu2p and XMAP215 homologues function on multiple types of microtubules within the cell. On the plus end of cytoplasmic microtubules, Stu2p functions in cytoplasmic microtubule orientation to facilitate positioning of the mitotic spindle (Kosco et al., 2001). XMAP215 is a dynamic component of the kinetochore that functions in metaphase

Abbreviations: AD, activation domain; BD, DNA binding domain; MAP, microtubule-associated protein; SC, synthetic complete; SPB, spindle pole body; STUbL, SUMO-Targeted Ubiquitin Ligase; TBS, Tris buffered saline; YPD, yeast peptone dextrose.

TABLE 1 Strains and plasmids used in this study

Yeast strains	Genotype/comments	Source
yRM1756/PJ69-4α	*MATα trp1–901 leu2–3 leu2–112 ura3–52 his3Δ200 gal4Δ gal80Δ LYS2::GAL1-HIS3 GAL2-ADE2 met2::GAL7-lacZ*	(James et al., 1996)
yRM1757/PJ69-4A	*MATa trp1–901 leu2–3 leu2–112 ura3–52 his3Δ200 gal4Δ gal80Δ LYS2::GAL1-HIS3 GAL2-ADE2 met2::GAL7-lacZ*	(James et al., 1996)
yRM2057	*MATa bim1Δ::KAN trp1–901 leu2–3 leu2–112 ura3–52 his3Δ200 gal4Δ gal80Δ LYS2::GAL1-HIS3 GAL2-ADE2 met2::GAL7-lacZ*	(Miller et al., 2000)
yRM2122/pCUY1147	*MATa PAce1-UBR1 PAce1-ROX1 trp1-Δ1 ade2–101 ura3–52 lys2–801 stu2Δ::URA3::P_{Anb1}UB-R-STU2*	(Kosco et al., 2001)
yRM2123/pCUY1148	*MATa PAce1-UBR1 PAce1-ROX1 trp1-Δ1 ade2–101 lys2–801 ura3–52::URA3*	(Kosco et al., 2001)
yRM2146/MS52	*MATα ura3–52 leu2–3 leu2–112 trp1Δ1*	(Miller et al., 1999)
yRM2258	*MATa bik1Δ::TRP1 trp1–901 leu2–3 leu2–112 ura3–52 his3Δ200 gal4Δ gal80Δ LYS2::GAL1-HIS3 GAL2-ADE2 met2::GAL7-lacZ*	(Moore et al., 2006)
yRM6172	*MATa kar9Δ::KAN trp1–901 leu2–3 leu2–112 ura3–52 his3Δ200 gal4Δ gal80Δ LYS2::GAL1-HIS3 GAL2-ADE2 met2::GAL7-lacZ*	(Meednu et al., 2008)
yRM6249	*MATa pac1Δ::KAN trp1–901 leu2–3 leu2–112 ura3–52 his3Δ200 gal4Δ gal80Δ LYS2::GAL1-HIS3 GAL2-ADE2 met2::GAL7-lacZ*	(Alonso et al., 2012)
yRM7230	*MATα ura3–52 leu2–3 leu2–112 trp1Δ* [*pRM6956 pGAL-STU2-TAP (tag is his6-HA–protein A) URA3 Amp^R*]	This Study
yRM8011/YOK428	*MATα ulp1::KAN his3Δ1 leu2Δ ura3Δ [ulp1-TS- NAT-TRP1] [pRS425 GPD- flag-SMT3-GG LEU2 2μ Amp^R]*	(Elmore et al., 2011)
yRM8012/YOK430	*MATα ulp1::KAN his3Δ1 leu2Δ ura3Δ [ulp1-TS- NAT-TRP1] [pRS425 GPD-SMT3-GG LEU2 2μ Amp^R]*	(Elmore et al., 2011)
yRM8139	*MATα ulp1::KAN his3Δ1 leu2Δ ura3Δ [ulp1-TS- NAT-TRP1]*	(Alonso et al., 2012)
yRM9417	*MATa STU2-his6::HIS3 met15Δ his3Δ leu2Δ ura3Δ*	This study
yRM9909	*MATa trp1–901 leu2–3 leu2–112 ura3–52 his3Δ200 gal4Δ gal80Δ LYS2::GAL1-HIS3 GAL2-ADE2 met2::GAL7-lacZ*	(James et al., 1996)
yRM10637	*MATa his3Δ leu2Δ met15Δ ura3Δ* [pRM2119 *STU2–3xHA* Cen6 *LEU2* Amp^R]	This study
yRM10641	*MATa his3Δ met15Δ ura3Δ leu2Δ [pRM2200 YCP LEU2+* Amp^R]	This study
yRM10782/yKU5	*MATa NIS1–6xHA::TRP1*	(Uzunova et al., 2007)
Plasmids		
pRM1151	*pGAD-C1 empty GAL4-AD LEU2 2μ* Amp^R	(James et al., 1996)
pRM1154	*pGBDU-C1 empty GAL4-AD URA3 2μ* Amp^R	(James et al., 1996)
pRM1157	*pGBD-C1 empty GAL4-AD TRP1 2μ* Amp^R	(James et al., 1996)
pRM1493	*GBDU-KAR9 URA3 2μ* Amp^R	(Miller et al., 2000)
pRM1916	*PGAD-STU2-aa649–888 LEU2 2μ* Amp^R	(Miller et al., 2000)
pRM2095	*pGBD-TUB1 CEN* Amp^R *TRP1*	D. Botstein/this study
pRM2096	*pGBD-TUB3 CEN* Amp^R *TRP1*	D. Botstein/this study
pRM2117	*pGAD-TUB2-m CEN* Amp^R *LEU2*	D. Botstein /this study
pRM 2119/WP70	*STU2–3xHA* Cen6 *LEU2* Amp^R	(Wang and Huffaker, 1997)
pRM2200/pRS415	*LEU2 CEN* Amp^R	(Sikorski and Hieter, 1989)
pRM2205/pRS426	*URA3 2μ* Amp^R	(Sikorski and Hieter, 1989)
pRM2627	*GAD-BIK1 LEU2 2μ* Amp^R	(Moore et al., 2006)
pRM2759	GST Amp^R	(Moore et al., 2006)

(Continues)

TABLE 1 (Continued)

Yeast strains	Genotype/comments	Source
pRM2908	*pGAL URA3 2μ* Amp^R	This study
pRM3595	*GBDU-KIP2 URA3 2μ* Amp^R	(Meednu et al., 2008)
pRM3604	GBDU-PAC1 URA3 2μ Amp^R	This study
pRM4380	*GAD424 LEU2 2μ* Amp^R	(Meednu et al., 2008)
pRM4382/pLAJ20	GAD-SMT3-GG LEU2 2μ Amp^R	(Meednu et al., 2008)
pRM4383/pLAJ21	GAD-SMT3-GA LEU2 2μ Amp^R	(Meednu et al., 2008)
pRM4495	GAD-UBC9 LEU2 2μ Amp^R	(Meednu et al., 2008)
pRM4496	GAD-NFI1 LEU2 2μ Amp^R	(Meednu et al., 2008)
pRM4595	GAD-NIS1 LEU2 2μ Amp^R	(Meednu et al., 2008)
pRM4596	GAD-RIS1/ULS1 LEU2 2μ Amp^R	(Meednu et al., 2008)
pRM4597	GAD-WSS1 LEU2 2μ Amp^R	(Meednu et al., 2008)
pRM4920/pLAJ19	GAD-SMT3 LEU2 2μ Amp^R	(Meednu et al., 2008)
pRM4924	GBDU-BIK1 URA3 2μ Amp^R	This study
pRM5169	his6-UBC9 Amp^R	(Johnson and Blobel, 1997)
pRM5251	pGAL-3HA-FLAG-SMT3 HIS3 Amp^R	This study
pRM6713	his6-S-tag-Smt3p-GG Kan^R	This study
pRM6760	GST-AOS1/UBA2 2μ Amp^R	(Bencsath et al., 2002)
pRM6956	pGAL-STU2-TAP (tag consists of his6- HA-protein A) URA3 Amp^R	(Gelperin et al., 2005)
pRM7228	BD-STU2 aa1–658 URA3 2μ Amp^R	This study
pRM7247/pCUB495	BD-STU2 TRP+ 2μ Amp^R	(Wolyniak et al., 2006)
pRM9370	BD-STU2 aa613–888 URA3 2μ Amp^R	This study
pRM9426	BD-STU2 URA3 2μ Amp^R	This study
pRM10097	GST-SUMO-GA Amp^R	This study
pRM10749	*GBD-TUB2-m CEN* Amp^R *TRP1*	D. Botstein/this study
pRM10785	BD-STU2 aa540–888 URA3 2μ Amp^R	This study
pRM10787	BD-STU2 aa540–801 URA3 2μ Amp^R	This study
pRM10792	BD-STU2 aa540–657 URA3 2μ Amp^R	This study
pRM10818	SUMO-GST Amp^R	This study
pRM11115	BD-STU2 aa613–801 URA3 2μ Amp^R	This study

chromosome alignment by helping to attach microtubules to the kinetochore (Aravamudhan, Felzer-Kim, Gurunathan, & Joglekar, 2014; Kitamura et al., 2010; Ma, McQueen, Cuschieri, Vogel, & Measday, 2007). In addition to regulating microtubule dynamics, the yeast Stu2p can stabilize tension-bearing microtubule attachments at the kinetochore (Miller, Asbury, & Biggins, 2016). Stu2p, like other XMAP215 members, is a component of the MTOC and interacts with TACC complex proteins (Al-Bassam & Chang, 2011; Wang & Huffaker, 1997). While the role of Stu2p at the yeast MTOC remains unclear, it is known that XMAP215 can promote microtubule nucleation (Wieczorek, Bechstedt, Chaaban, & Brouhard, 2015).

The signal transduction systems that regulate the various functions of Stu2p and TOG proteins are not well understood. Stu2p can be modulated by phosphorylation (Park et al., 2008). The phosphorylation of TOG binding-partner proteins is also a mode of regulating its localization and activity in *Drosophila* & fission yeast (Okada, Toda, Yamamoto, & Sato, 2014; Trogden & Rogers, 2015). However, less is known about the regulation of Stu2p by other types of post-translational modifications. In this paper, we show that Stu2p interacts with the small ubiquitin-like modifier termed SUMO, encoded by *SMT3*.

The SUMO moiety is well known to attach to lysine residues through the action of an E2 conjugation enzyme and an E3 ligase (reviewed in Gareau & Lima, 2010 and Alonso et al., 2015). Unlike ubiquitin which utilizes numerous E2 enzymes, sumoylation uses a single E2 enzyme, called Ubc9p (Johnson & Blobel, 1997; Kerscher,

Felberbaum, & Hochstrasser, 2006). In contrast to higher eukaryotes which has three families of E3 enzymes with multiple members in each, there are only three confirmed E3 enzymes for sumoylation in yeasts, the best characterized of which are Siz1p and Nfi1p/Siz2p (Johnson & Gupta, 2001; Pichler, Fatouros, Lee, & Eisenhardt, 2017; Takahashi, Kahyo, Toh, Yasuda, & Kikuchi, 2001). Attachment of SUMO to target proteins is reversible through the action of two SUMO specific proteases, Ulp1p and Ulp2p (Bylebyl, Belichenko, & Johnson, 2003; Kroetz & Hochstrasser, 2009; Li & Hochstrasser, 1999, 2000). The WLM metalloprotease Wss1p is thought to remove SUMO from targets (Mullen, Chen, & Brill, 2010), but may remove ubiquitin as well (Su & Hochstrasser, 2010).

SUMO can interact with a partner protein in two ways, covalently or noncovalently. For covalent interactions, SUMO is often attached to the lysine residue within the canonical consensus site, ϕKXD/E, where ϕ is a hydrophobic residue and X can be any amino acid. However, degenerate consensus sites are also used frequently, which can confound the identification of modified lysines (Hendriks et al., 2017). SUMO can also interact non-covalently with a protein. This occurs though the conserved SUMO Interacting Motif (SIM) found in SUMO's binding partners. The SIM motif consists of a stretch of hydrophobic amino acids in the pattern (I/L/V) X (I/L/V) (I/L/V) with the X position being occupied by any amino acid (Kroetz & Hochstrasser, 2009; Song, Durrin, Wilkinson, Krontiris, & Chen, 2004), although the consensus sequence may be more complex (Jardin, Horn, & Sticht, 2015).

In this work, we show that Stu2p/XMAP215 interacts both covalently and non-covalently with SUMO, as well as with the SUMO-targeted ubiquitin ligase (STUbL), Ris1p. A major binding partner of Stu2p is the tubulin dimer. Here, we show that beta-tubulin encoded by *TUB2* also interacts with SUMO and Ris1p.

2 | RESULTS

2.1 | Stu2p interacts with SUMO and the SUMO machinery

Stu2p is important for spindle positioning (Kosco et al., 2001). Stu2p also interacts with several other microtubule-associated proteins, including the spindle positioning protein Kar9p, the CLIP-170 homologue Bik1p, the EB1 homolog Bim1p, and the kinetochore protein Ndc80p (Alonso et al., 2015; Blake-Hodek, Cassimeris, & Huffaker, 2010; Miller, Cheng, & Rose, 2000; Wolyniak et al., 2006; Wong et al., 2007). Each of these interacts with SUMO (Alonso et al., 2012; Leisner et al., 2008; Meednu et al., 2008; Montpetit, Hazbun, Fields, & Hieter, 2006). Therefore, we tested whether *STU2* might also interact with SUMO using a two-hybrid assay. For this, we employed three forms of SUMO; a full-length SUMO, a preprocessed form in which the terminal three amino acids were removed from the coding DNA (*SUMO*-GG), and a conjugation incompetent form SUMO in which the glycine used in conjugation was mutated to an alanine (SUMO-GA). As shown in Figure 1a, *STU2* interacted with full-length SUMO and with SUMO-GG, but not with SUMO-GA.

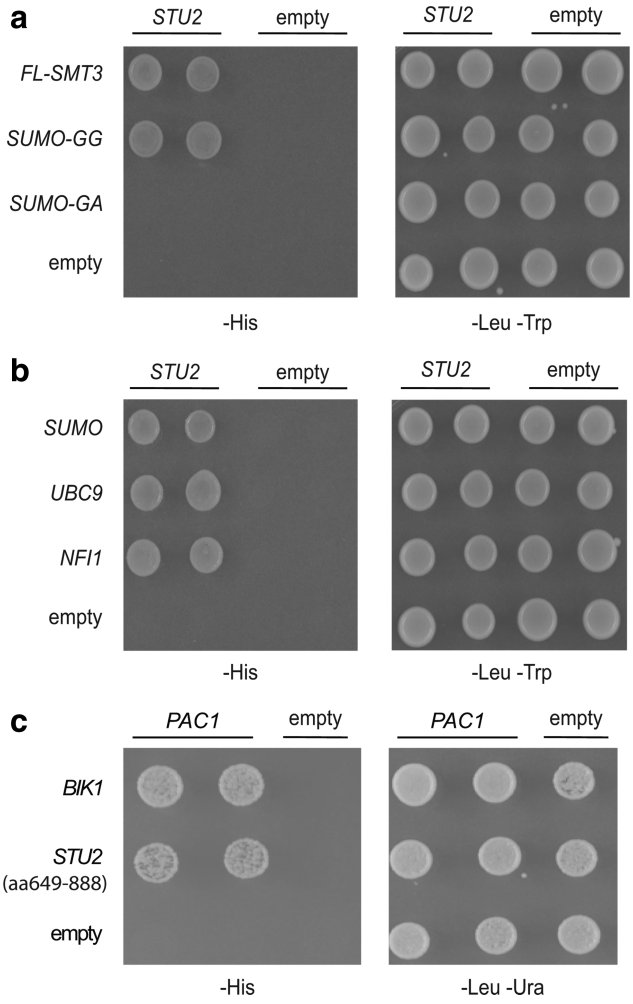

FIGURE 1 *STU2* interacts with the sumoylation machinery and *PAC1/Lis1* by two-hybrid analysis. (a). *STU2* interacts with SUMO-GG but not SUMO-GA. Two-hybrid reporter strains were generated by transforming either BD-*STU2* (pRM7247), empty-BD (pRM1154) and AD-FL-SUMO (pRM4920), AD-SUMO-GG (pRM4382), *or* SUMO-GA (pRM4383), as described in Table 1. Transformants were selected on SC media lacking uracil and tryptophan (-ura -trp). Interaction was assayed by yeast growth on media lacking histidine (-his) as previously described (Alonso et al., 2012). Two independent colonies are shown for each interaction. (b) *STU2* interacts with multiple enzymes in the sumoylation pathway. BD-*STU2* (pRM7247) was tested for interaction with AD-SUMO (pRM4920), AD-*UBC9* (pRM4495), and AD-*NFI1* (pRM4496). (c) *STU2* interacts with *PAC1/Lis1*. BD-*PAC1* (pRM3604) was analyzed for interaction with AD-*STU2* (pRM1916). This encodes *STU2*-aa649–888. AD-*BIK1* (pRM2627) serves as a positive control

As conjugation of SUMO to a target protein requires several enzymes in the sumoylation pathway (Praefcke, Hofmann, & Dohmen, 2012), we asked whether *STU2* could interact with other components of the sumoylation pathway. We found that *STU2* interacted with the E2 conjugating enzyme encoded by *UBC9*, confirming a previous two-hybrid screen (Wong et al., 2007). Extending this observation, we also found that *STU2* interacted with the E3 ligase enzyme encoded by

NFI1/SIZ2 (Figure 1b). As discussed in more detail below, these two-hybrid interactions do not distinguish between covalent and non-covalent interactions between Stu2p and SUMO.

Conserved in yeast and mammalian systems, Pac1p/Lis1 interacts with Bik1p/CLIP-170 (Coquelle et al., 2002; Markus et al., 2011; Sheeman et al., 2003; Tai, Dujardin, Faulkner, & Vallee, 2002). Bik1p has previously been shown to interact with Stu2p (Wolyniak et al., 2006). We therefore tested whether *STU2* might also interact with *PAC1/Lis1*. As shown in Figure 1c, it does, confirming previous genomics reports (Wong et al., 2007). The *STU2* two-hybrid construct used in this analysis (*STU2*-aa649–888) lacks the two TOG domains, coding for only the dimerization and MAP domains of Stu2p. This finding suggests that the Stu2p-Pac1p interaction does not require the TOG domains of Stu2p. As Pac1p/Lis1 was recently demonstrated to be sumoylated, this represents the fifth sumoylated MAP with which Stu2p interacts (Alonso et al., 2012; Meednu et al., 2008; Montpetit et al., 2006).

The interaction of Pac1p/Lis1 with SUMO requires the presence of its binding partner Bik1p (Alonso et al., 2012), and vice versa. To ascertain whether Bik1p or other SUMO-interacting MAPs are necessary for Stu2p's interaction with SUMO, we tested *STU2*'s interaction with SUMO in two-hybrid reporter strains that were deleted for each of these MAPs. The interaction of Stu2p with SUMO was not altered in reporter strains deleted for *BIK1/CLIP-170*, *PAC1/LIS1*, or *BIM1/EB1* (Figure 2a-c). This suggests that Stu2p's interaction with SUMO does not require these MAPs. It also implies that Bik1p/CLIP-170, Bim1p/EB1 or Pac1/Lis1 do not serve a bridging function between Stu2p and SUMO. Kar9p is a cytoskeletal linker protein that orients microtubules for spindle positioning (Bloom, 2000; Gundersen & Bretscher, 2003; Lee et al., 2000; Liakopoulos, Kusch, Grava, Vogel, & Barral, 2003; Miller & Rose, 1998; Miller, Matheos, & Rose, 1999). Like Stu2p, it also plays a role at the kinetochore (Schweiggert, Stevermann, Panigada, Kammerer, & Liakopoulos, 2016). Kar9p interacts with Stu2p as well (Miller et al., 2000; Moore & Miller, 2007). Like Pac1p/Lis1 and Bim1p/EB1, Kar9p also was not required for Stu2p's interaction with SUMO. However, in the *kar9*Δ strain, Stu2p displayed reduced interactions with SUMO, with the E2 enzyme Ubc9p, the E3 enzyme Nfi1p, and the protease Wss1p. This suggests that Kar9p may facilitate the interaction of Stu2p with the sumoylation machinery (Figure 2d). Combined, these findings suggest that the interaction of SUMO with Stu2p is largely independent of several of its binding partners.

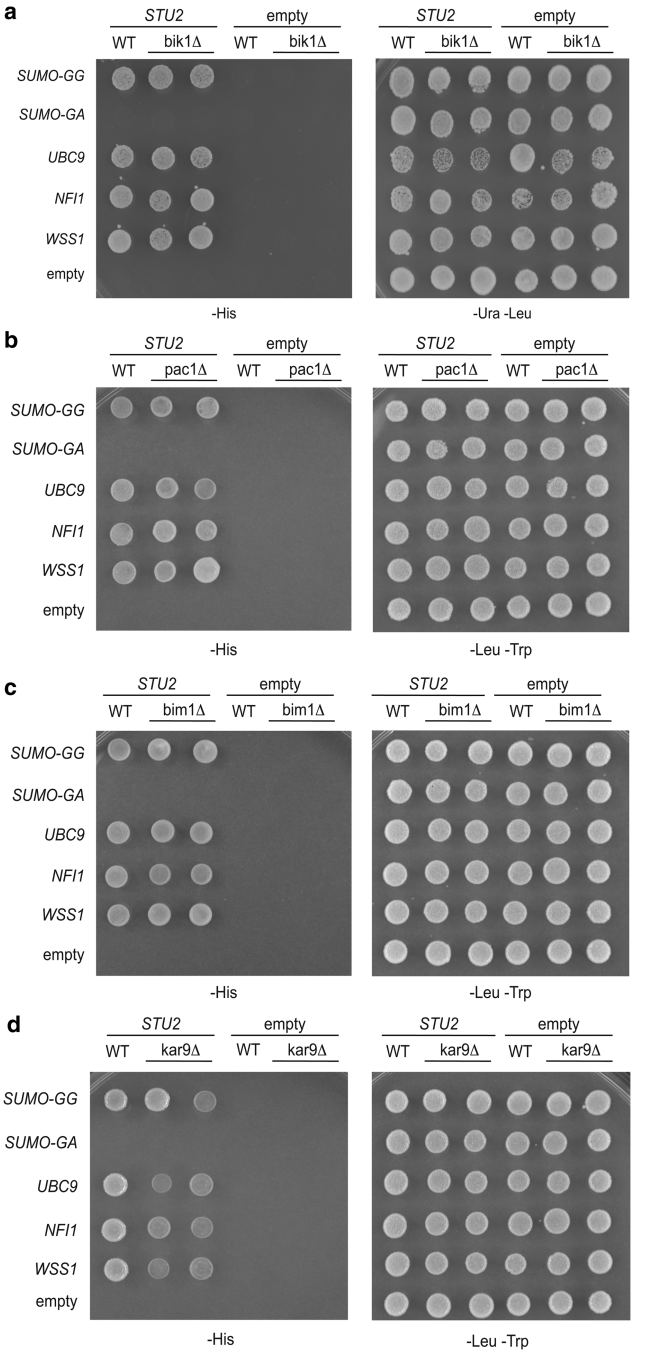

FIGURE 2 Bik1p/CLIP-170, Pac1p/Lis1, and Bim1p/EB1 are not required for Stu2p's interaction with SUMO, whereas Kar9p facilitates interactions between Stu2p and the sumoylation pathway. AD-SUMO-GG (pRM4382), AD-SUMO-GA (pRM4383), AD-*UBC9* (pRM4495), AD-*NFI1* (pRM4496), AD-*WSS1* (pRM4597), or empty-AD (pRM1151) were transformed into a two-hybrid reporter strain containing BD-*STU2* (pRM7247) or empty-BD (pRM1157). The reporter strains used were wild type (yRM1757), and strains deleted for *KAR9* (yRM6172), *BIM1/EB1* (yRM2057), or *PAC1/Lis1* (yRM6249). For the *bik1*Δ strain (yRM2258), the BD-*STU2* plasmid (pRM9426) and the empty BD (pRM1154) were used to meet auxotrophic selection requirements

2.2 | Amino acids 613–801, which encompass the dimerization domain of Stu2p, are necessary and sufficient for interaction with SUMO

Stu2p is composed of several well-characterized domains. Its two TOG domains are responsible for binding tubulin dimers (Al-Bassam et al., 2006; Widlund et al., 2011). The MT domain is involved in interaction with MT polymers (Wang & Huffaker, 1997). The Huffaker lab previously demonstrated that the dimerization domain is necessary and sufficient for Stu2p's interaction with itself (Wolyniak et al., 2006). The C-terminal MAP domain has been shown to be important for interactions with several MAPs (Miller et al., 2000; Wolyniak et al., 2006). To

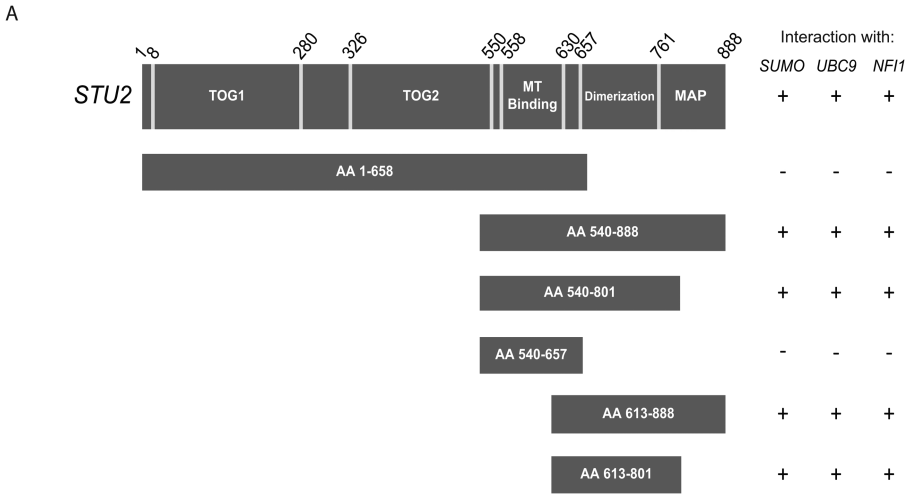

FIGURE 3 The dimerization domain of Stu2p interacts with SUMO. Two-hybrid interactions with AD-SUMO-GG (pRM4382), AD-*UBC9* (pRM4495) and AD-*NFI1* (pRM4496) were assayed using the indicated amino- and carboxy-terminal truncations of BD-*STU2* in the yeast reporter strain, pJ69-4A/yRM9909. A plus sign represents plasmid combinations that supported yeast growth. The following plasmids were used: pRM9426 encoding full-length *STU2* from amino acids 1–888, pRM7228 encoding amino acids 1–658, pRM10785 encoding amino acids 540–888, pRM10792 encoding amino acids 540–657, pRM10787 encoding amino acids 540–801, pRM9370 encoding amino acids 613–888, and pRM11115 encoding amino acids 613–801. Four independent colonies were tested for each truncation and compared each time to the full-length Stu2p

identify the regions of Stu2p that are required for interaction with SUMO and the sumoylation machinery, we created a series of N- and C- terminal truncations of Stu2p for two-hybrid analysis. When the region encoding the dimerization domain and the MAP- interaction domain was deleted, Stu2p interactions with SUMO and the sumoylation machinery were lost (Figure 3, AA 1–658). In contrast, when the TOG domains were deleted, the interaction with SUMO was retained (Figure 3, AA540–888). The two-hybrid construct lacking a significant portion of the MT binding domain but containing both the dimerization domain and the MAP domain (AA613–888) did interact with SUMO. In contrast, the construct containing the MT binding domain but lacking the Stu2p dimerization domain (AA540–657) did not interact. The AA613–801 construct expresses a portion of the microtubule binding domain, the dimerization domain, and 40 amino acids flanking the dimerization domain. This construct retained interactions with SUMO, Ubc9p, and Nfi1p. These data suggest that the TOG domains are not required for Stu2p's interaction with SUMO. These data also suggest that a region encompassing the dimerization domain is necessary and sufficient for Stu2p's interaction with SUMO and the sumoylation machinery. Consistent with this finding, predicted motifs for both covalent and non-covalent SUMO interactions are present in this region. A predicted site for SUMO conjugation (ϕxKE) resides at lysine 795. In addition, two potential SIMs ([I/L/V] [I/L/V] X [I/L/V]) reside at amino acids 636–639 (VLLT) and 738–741 (VLSL) (Zhao et al., 2014).

2.3 | Stu2p can be sumoylated *in vitro*

We next examined the possibility that SUMO could be attached to Stu2p using an *in vitro* sumoylation assay, described previously (Alonso et al., 2012; Meednu et al., 2008). For this, a Stu2-TAP tag fusion was purified from yeast and components of the sumoylation pathway including SUMO, Ubc9p and Aos1/Uba2p were purified from bacteria (Puig et al., 2001). SUMO was used in the processed form, SUMO-GG. In the reaction in which all the necessary components of the sumoylation pathway and ATP were included, four shifted bands were observed using anti-HA to detect Stu2-TAP (Figure 4, lane 1). When a conjugation-incompetent form of SUMO, SUMO-GA, was used in place of SUMO-GG, the shifted bands were not detected (Lane 7). Therefore, Stu2p can be sumoylated *in vitro* and the terminal glycine residue of SUMO is required for this *in vitro* sumoylation reaction.

2.4 | Stu2p interacts with the STUbL enzyme Ris1p, and copurifies with ubiquitin

STUbL enzymes frequently interact with sumoylated proteins to ubiquitinate them. We previously reported that Pac1p/Lis1 interacts with the STUbL enzyme Ris1p, the bud-neck interacting protein Nis1p, and the SUMO protease Wss1p (Alonso et al., 2012). To determine whether Stu2p displays a similar pattern of interactions, we tested for an interaction between Stu2p and these proteins by two-hybrid analysis. As shown in Figure 5a, they did interact. Because STUbL enzymes ubiquitinate their targets, we next tested for a direct interaction between Stu2p and ubiquitin. We immunoprecipitated ubiquitin and analyzed the precipitate for the presence of Stu2p by western blotting. As shown in Figure 5b, Stu2p copurified with ubiquitin, but not the vector control.

2.5 | SUMO and Stu2p copurify

To investigate whether the higher molecular weight forms of Stu2p observed *in vitro* are present *in vivo*, whole-cell extracts from a *ulp1*-ts

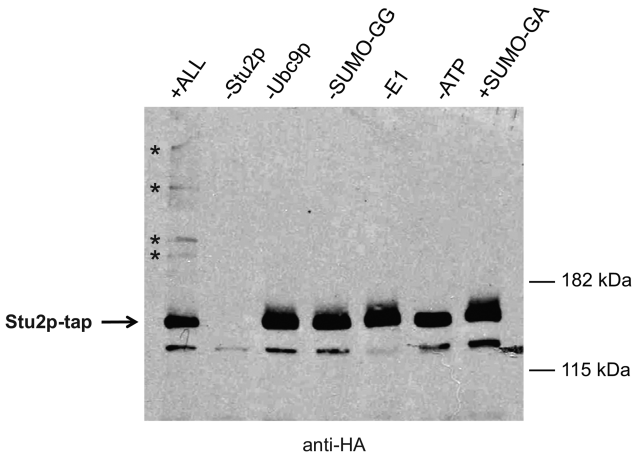

FIGURE 4 Stu2p can be conjugated by SUMO *in vitro*. Stu2p-TAP (pRM6956) was purified from yeast using nickel column chromatography. The purified protein was incubated with purified components necessary for sumoylation, SUMO-GG (pRM6713), Ubc9p (pRM5169), and Aos1p/Uba2p (pRM6760) in the presence of ATP and an ATP regeneration system (lane 1), as described in Materials and Methods. As controls, each of the required components of the reaction was omitted from the reaction as follows: Stu2p (lane 2), SUMO-GG (lane 3), Ubc9p (lane 4), Aos1/Uba2p (E1) (lane 5) and ATP (lane 6). In the last reaction, SUMO-GG was replaced by SUMO-GA (lane 7), a mutated form of SUMO in which the essential glycine for conjugation is changed to alanine. Anti-HA was used to detect Stu2p. The shifted bands that are recognized by anti-HA (*) are specific to lane 1 when all the essential components are present

yeast strain expressing Stu2-HA were used in a pull-down using anti-HA agarose beads and blotted for SUMO. At least one higher molecular-weight form of Stu2-HA coimmunoprecipitated with SUMO (Figure 6a). To examine this using the reciprocal approach, we pulled down SUMO using a SUMO antibody and then blotted for Stu2-HA. Stu2p coimmunoprecipitated with SUMO (Figure 6b). These coimmunoprecipitation results could in theory be the result of a co-immunoprecipitation of another SUMO-modified protein that co-migrates at the same molecular weight as Stu2p. To eliminate this possibility, we sought to determine if SUMO would coisolate with Stu2p under denaturing conditions. Genomic Stu2-his6 solubilized in 8M urea was enriched on nickel-NTA agarose, and eluted with sample buffer. Western blot analysis revealed that the slower migrating Stu2p band was immuno-reactive with anti-SUMO (Figure 6c). These findings suggest that SUMO is conjugated to Stu2p.

2.6 | Stu2p binds noncovalently to SUMO

It is well known that SUMO can be conjugated to and also bind noncovalently to target proteins. For example, the kinesin CENP-E can interact non-covalently with SUMO and also be conjugated by it (Zhang et al., 2008). To investigate whether Stu2p might bind noncovalently to SUMO, we assayed for an interaction using two forms of SUMO that are incompetent to form an isopeptide bond. In the first construct, GST-SUMO-GA, the terminal glycine of SUMO, glycine 98, was mutated to the conjugation incompetent residue, alanine. In the second construct, SUMO-GST, the terminal glycine of SUMO was fused in frame with the amino terminus of GST in a standard peptide bond, blocking the access of the carboxyl group of the terminal glycine for conjugation. Both constructs were expressed in bacteria and purified on glutathione beads. To test for a non-covalent interaction, yeast extracts were incubated with the two SUMO fusions. As a positive control, Nis1p, a protein known to interact non-covalently with SUMO, was included in the analysis (Uzunova et al., 2007). It was retained on both versions of the SUMO column (Figure 7a). In contrast, Stu2-HA was retained on only the GST-SUMO-GA column. These findings suggest that Stu2p interacts noncovalently with SUMO and that this interaction is restricted to one orientation of SUMO.

2.7 | Tubulin interacts with SUMO noncovalently

The major binding partner of Stu2p is tubulin. We therefore asked whether tubulin might also bind to SUMO. To answer this question, an

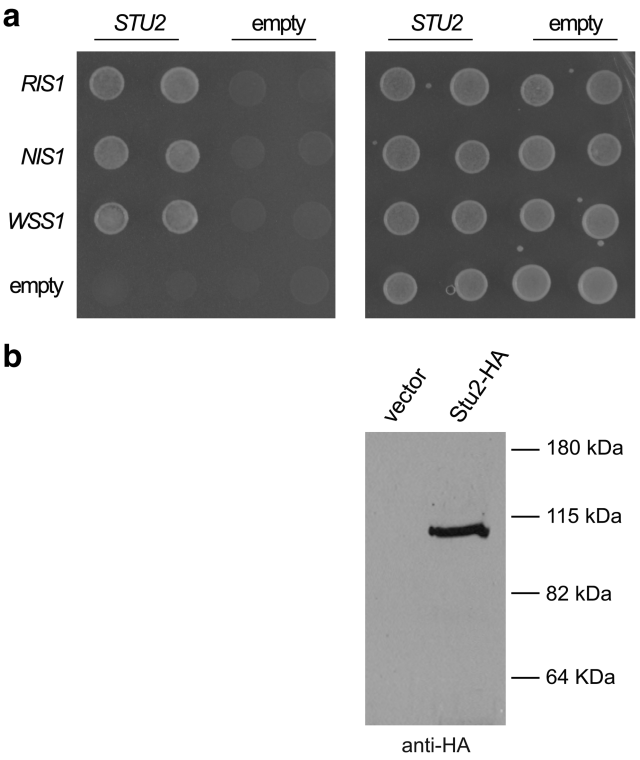

FIGURE 5 (a) Stu2p interacts with the STUbL enzyme Ris1p, the neck-interacting protein Nis1p, and the SUMO isopeptidase Wss1p by two-hybrid analysis. BD-*STU2* (pRM9426) was tested for interaction against the weak suppressor of SUMO encoded by AD-*WSS1* (pRM4597), AD-*RIS1* (pRM4596), AD-*NIS1* (pRM4595), or empty-AD (pRM4380). Transformants were selected on media lacking uracil and leucine (-ura -leu) and assayed for interactions on media lacking histidine (-his). (b) Stu2p co-IPs with ubiquitin. Plasmids expressing Stu2-HA (pRM2119) or vector (pRM2200) where transformed into a *ulp1-TS* strain (yRM8139). Whole-cell lysates were prepared, as described in Materials and Methods. Ubiquitin was immunoprecipitated with anti-ubiquitin and the precipitate was blotted with anti-Stu2p, as described in Materials and Methods

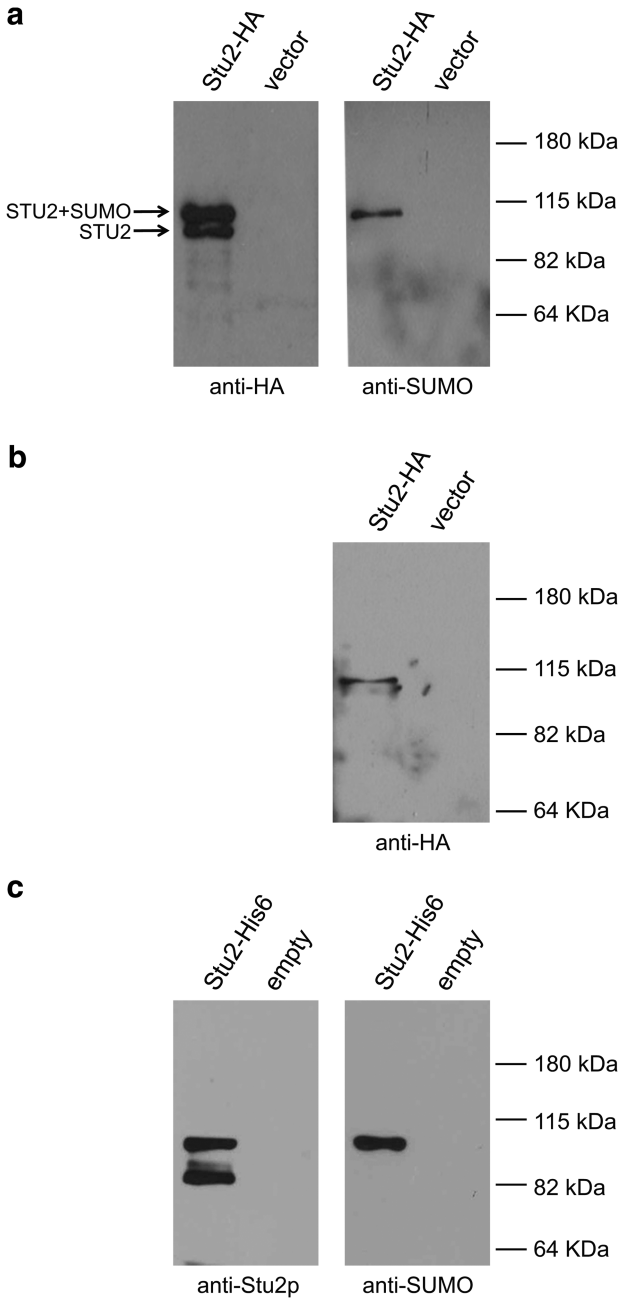

FIGURE 6 (a) SUMO co-IPs with Stu2p. Plasmid expressing Stu2-HA (pRM2119) or vector (pRM2200) where transformed into a *ulp1-TS* strain (yRM8139). Whole-cell lysates were prepared from cultures grown overnight to saturation, as described in Materials and Methods. Stu2-HA was immunoprecipitated using mouse anti-HA agarose beads (Sigma-Aldrich). The western blot was probed with rabbit anti-HA (Sigma-Aldrich). (b) Stu2p co-IPs with SUMO. SUMO was immunoprecipitated with anti-SUMO (Rockland, Inc. Gilbertsville, PA) from a *ulp1-TS* strain (yRM8139) containing Stu2-HA (pRM2119), or an empty vector, as described in Materials and Methods. The blot was probed with mouse anti-HA (Sigma-Aldrich). Saturated overnight cultures were used to prepare whole-cell extracts. (c) Stu2-his6 co-isolates with SUMO under denaturing conditions. Yeast whole-cell extracts containing Stu2-his6 (yRM9417) where incubated with Ni-NTA agarose in the presence of 8M urea. To analyze bands for co-reactivity, identical blots where probed with rabbit anti-Stu2p and anti-SUMO

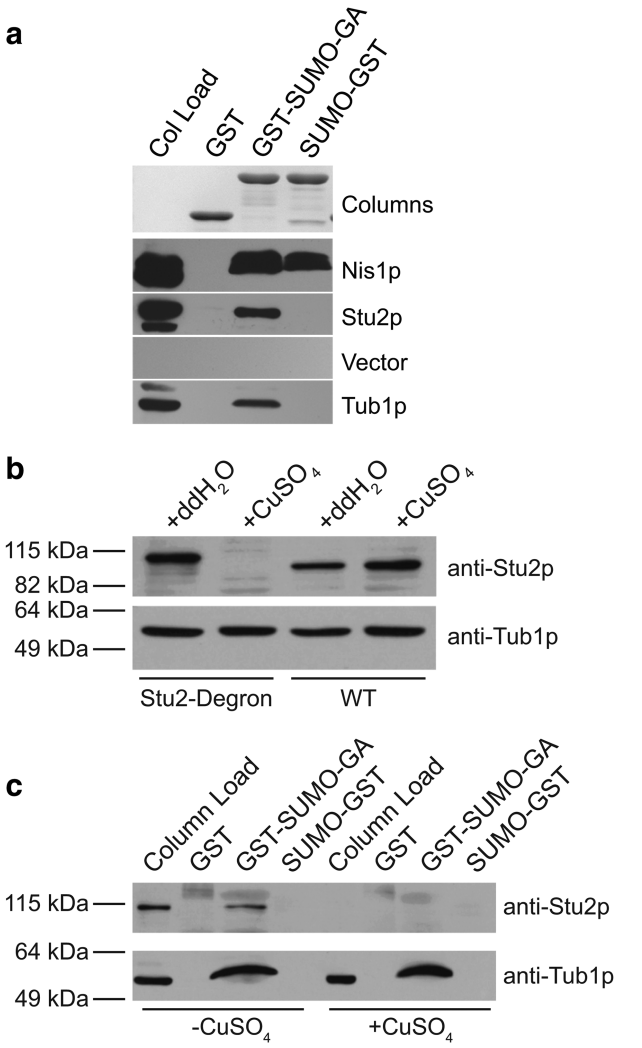

FIGURE 7 (a) Stu2p and tubulin bind non-covalently to SUMO. Columns of GST-SUMO-GA (pRM10097), SUMO-GST (pRM10818), or GST alone (pRM2759) were incubated with whole-cell extracts prepared from cells expressing Stu2-HA (yRM10637), Nis1-HA (yRM10782) or empty vector (yRM10641), as described in Material and Methods. Bound proteins were eluted with Laemmli sample buffer and analyzed by immunoblotting. 1/20 of the GST columns are shown in the Coomassie blue stained panel labeled "Columns." To detect the HA epitope of Stu2-HA and Nis1-HA, mouse anti-HA (Santa Cruz Biotechnology, Santa Cruz, CA) was used. To detect tubulin, rat anti-alpha-tubulin (YOL 1/34, Accurate Biochemical, Westbury, NY) was used. To normalize for the different cellular abundance of the two proteins, 1/13th (150 μg) of the column load is shown for Nis1-HA and 1/215th (50 μg) of the column load is shown for the Stu2-HA extracts. (b) Stu2 is depleted in the degron shut-off strain. Wild type (yRM2123) and a Stu2-degron strain (yRM2122) were treated with or without 500 μM CuSO4 for 6.5 hr as described (Kosco et al., 2001). Whole-cell extracts were prepared as described in Materials and Methods. Samples were prepared for SDS-PAGE and western blotting with rabbit anti-Stu2p. Anti-tubulin was used as a loading control. (c) Tubulin binds GST-SUMO-GA in the absence of Stu2p. Whole-cell extracts were prepared from the Stu2-degron strain treated with or without copper sulfate as described Materials and Methods. SUMO columns were prepared as described in panel (a). Western blots were developed as described in panel (a)

identical nitrocellulose membrane was blotted with anti-Tub1p. As shown in Figure 7a, tubulin does bind to the GST-SUMO-GA column. Notably, we observed little or no binding by tubulin to the SUMO-GST or GST alone columns. However, this experiment does not differentiate between a direct or indirect binding of tubulin through a Stu2p bridge. To determine whether tubulin would bind when Stu2p was not present in the extract, we employed the degron-tagged Stu2p previously described by Kosco et al. (2001), and confirmed the "shut-off" of Stu2p in the presence of copper sulfate (Figure 7b). When Stu2p was "shut off," tubulin still bound to the column (Figure 7c). These findings suggest that Stu2p is not required for the interaction of tubulin with SUMO.

2.8 | Tubulin interacts with SUMO and a SUMO-targeted ubiquitin ligase by two-hybrid analysis

Considering that the tubulin dimer is comprised of an alpha and beta subunit, we next wanted to know whether interactions with SUMO could be detected with these tubulin subunits using two-hybrid analysis. Whereas alpha-tubulin two-hybrid constructs are viable, overexpression of beta-tubulin two-hybrid constructs is toxic to the cell. To overcome this limitation, we used a mutated form of beta-tubulin with lower toxicity for these experiments (a kind gift from Kristy Schwartz and David Botstein). Using this construct, we found that the beta-tubulin Tub2p interacted with both SUMO and the E3 enzyme Nfi1p (Figure 8a). The two alpha-tubulins in yeast, Tub1p and Tub3p, also interacted with Nfi1p, but displayed minimal interaction with SUMO. None of the tubulins interacted with the E2 conjugating enzyme Ubc9p (Figure 8a). It is notable that the interaction between beta-tubulin and SUMO was resistant to treatment with the microtubule-destabilizing drug, benomyl (Figure 8b). The interaction between the alpha-tubulins and Nfi1p was greatly decreased by the benomyl treatment but not by the DMSO solvent-alone control (Figure 8b,c). In contrast, the interaction of beta-tubulin and Nfi1p was resistant to benomyl treatment.

Because Stu2p interacts with the STUbL enzyme Ris1p (Figure 5), we asked whether the tubulins might also interact with Ris1p. While both alpha-tubulins interacted with the beta-tubulin fusion protein as expected, treatment with benomyl disrupted their interactions, thus serving as a positive control for the functionality of benomyl in this assay. This analysis revealed that Ris1p interacted with all three tubulins, Tub1p, Tub3p, and Tub2p (Figure 9a). Notably, the interactions between the alpha-tubulins and Ris1p were sensitive to benomyl, whereas the beta-tubulin displayed only a slight sensitivity (Figure 9b). In contrast, the Nis1p protein interacted most strongly with beta-tubulin, and only weakly with alpha-tubulins (Figure 9a). These interactions were eliminated by benomyl treatment. In all of these analyses, the alpha tubulins, Tub1 and Tub3p, displayed concordant results. These findings suggest that SUMO interacts better with beta-tubulin than with alpha-tubulins. This raises questions of whether the interactions of alpha-tubulins with SUMO are bridged by their dimer partner, beta-tubulin.

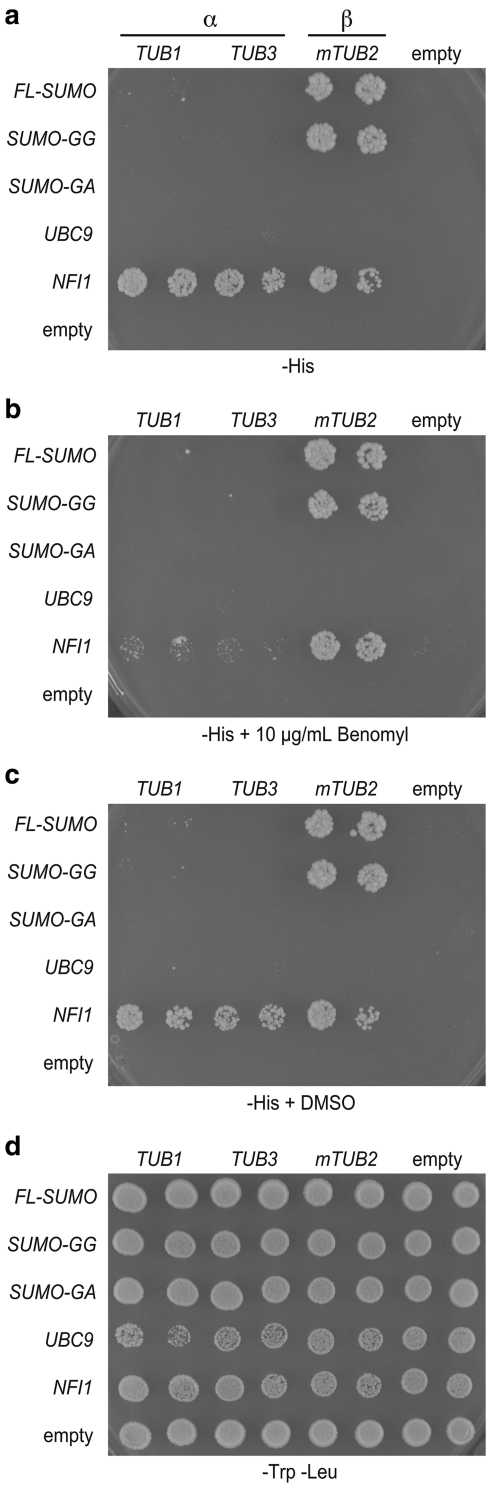

FIGURE 8 Beta-tubulin interacts with SUMO. (a). Alpha- and beta-tubulins fused to the *GAL4* DNA-binding domain (pRM2095, pRM2096, and pRM10749) were tested for interaction with AD-FL-SUMO, (pRM4920), AD-SUMO-GG (pRM4382), AD-SUMO-GA (pRM4383), AD-*UBC9* (pRM4495), and AD-*NFI1* (pRM4496), and empty-AD (pRM1151), as described above. Haploids were selected on media lacking uracil and tryptophan (-ura -trp) (d), and assayed for interactions on media lacking histidine (-his). Cells were simultaneously transferred to -his plates containing 10 µg mL^{-1} of benomyl (b) or an equivalent concentration of the DMSO solvent (c). Two independent colonies of each are shown

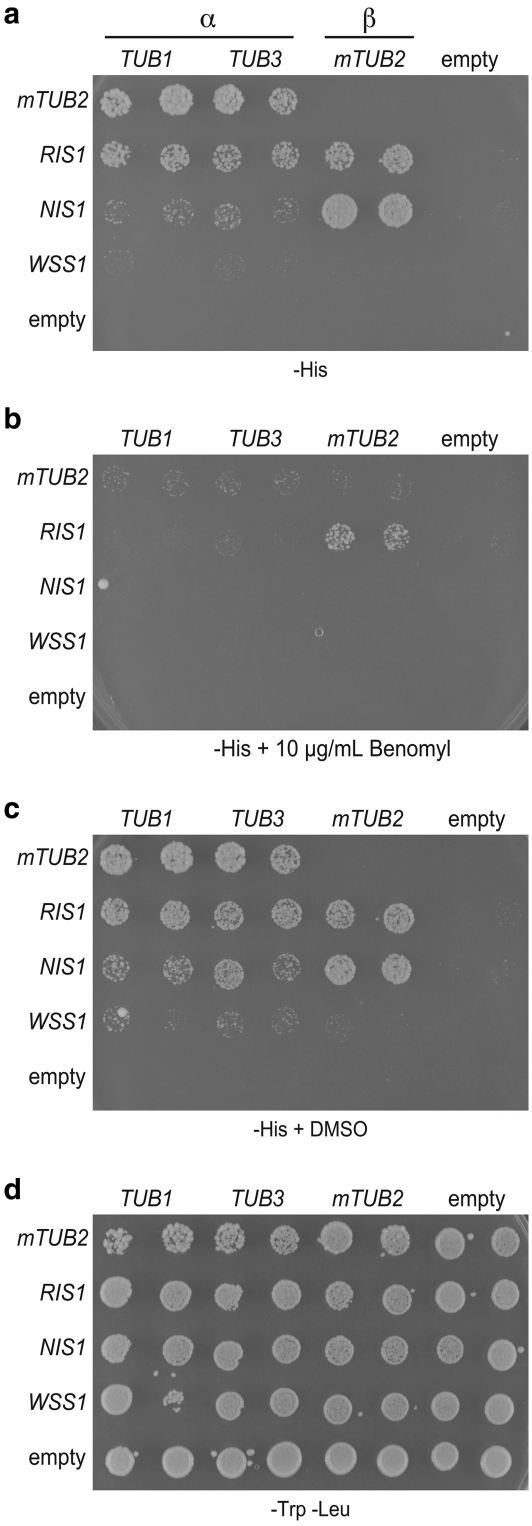

FIGURE 9 Alpha- and beta- tubulins interact with the STUbL enzyme, Ris1p. Alpha and beta-tubulins fused to the *GAL4* binding domain (pRM2095, pRM2096, and pRM10749) were tested for interaction with the STUbL enzyme AD-*RIS1* (pRM4596), AD-*NIS1* (pRM4595), AD-*WSS1* (pRM4597) or empty-AD (pRM4380), as described above. Cells were simultaneously transferred to -his plates containing 10 μg mL^{-1} of benomyl (b), or an equivalent concentration of the DMSO solvent (c). Two independent colonies of each are shown

3 | DISCUSSION

In this report, we present evidence that the microtubule polymerizing protein, Stu2p, interacts with SUMO and several enzymes in the sumoylation pathway. A major function of Stu2p is to promote tubulin-dimer addition onto microtubule plus-ends. Here, we also provide evidence for interactions between tubulin and SUMO.

Our data suggest that Stu2p-SUMO interactions occur by two distinct mechanisms, covalent and non-covalent. The hypothesis that the interaction has a covalent modality is supported by the finding that Stu2p copurifies with SUMO and vice versa. Further, the Stu2p band is reactive with anti-SUMO, even when purified in the presence of a strong denaturant. Stu2p can also be conjugated by SUMO in an *in vitro* assay. However, despite several attempts by mutagenesis and mass spectrometry, we have not yet been able to identify a lysine that is modified. We speculate that this is because of poor ion-mobility of sumoylated peptides in the mass spectrometer. Also, the sumoylated lysine residue may reside outside of the peptide fingerprint generated by the tryptic digestion that we used.

We have previously posited a model for the regulation of the MAP Pac1p/Lis1 by STUbLs and the proteasome (Alonso et al., 2012). Consistent with this model, we show that Stu2p also interacts with the STUbL enzyme Ris1p and ubiquitin. Thus, it is possible that SUMO signals for the rapid degradation of a particular subpopulation of Stu2p by the proteasome. Consistent with this, we have seen a higher molecular-weight band of Stu2p that is present in strains with lower levels of SUMO, but disappears with increasing levels of cellular SUMO (Supporting Information Figure S1).

In the noncovalent binding experiments, Stu2p bound much better to the SUMO-GA than the SUMO-GST column. This result is informative, since one would expect the SUMO-GST configuration to more accurately model the architecture of a sumoylated substrate than the SUMO-GA. Nevertheless, this differential binding suggests that Stu2p interacts with SUMO in an orientation-specific manner. Although the alpha-helix and beta-sheet in SUMO that are responsible for interactions with SIMs should be accessible in both constructs, it is likely that steric hindrance imposed by the GST reveals this specificity (Hecker, Rabiller, Haglund, Bayer, & Dikic, 2006; Jardin et al., 2015; Newman et al., 2017). Further, these results demonstrate that Stu2p can bind noncovalently to SUMO.

It should be noted that Stu2p's biochemical non-covalent binding to GST-SUMO-GA represents an inconsistency with our two-hybrid results, in which BD-*STU2* did not interact with an AD-SUMO-GA construct. In theory, the SUMO-GA mutation should eliminate only the covalent interactions between Stu2p and SUMO, leaving the non-covalent interactions intact. Yet in the two-hybrid analysis, no interaction is observed between Stu2p and SUMO-GA. It should also be noted that the biochemical assays used a C-terminal tag (Stu2-HA) in contrast to the amino-terminal BD fusion (DB-*STU2*) used in the two-hybrid assay. Thus, this difference could reflect an inhibitory effect conferred by the BD fusion to Stu2p that might yield a weaker or nondetectable interaction for the GA construct in the yeast two-hybrid assay.

This work extends previous work suggesting that Stu2p may interact with SUMO. Stu2p was seen to interact with SUMO using a high-throughput bi-fluorescence complementation (BiFC) assay (Sung et al., 2013) and a high throughput proteomics screen (Hendriks et al., 2017). These data suggest a covalent interaction, consistent with our data.

Our domain mapping identified a necessary and sufficient region that supports interactions between Stu2p and SUMO (Figure 3). This domain coincides with the domain responsible for Stu2p dimerization (Wolyniak et al., 2006). This domain of Stu2p also is required for its recruitment to the kinetochore and SPB (Haase et al., 2018). As SUMO is known to regulate the dimerization of several of its targets (Bossis et al., 2005; Rojas-Fernandez et al., 2014), we are currently working to determine whether SUMO regulates the dimerization of Stu2p. Indeed, the mechanisms regulating Stu2's coiled-coil formation remain to be elucidated. Several highly conserved lysine residues and two SIM motifs reside within this domain (Haase et al., 2018).

With this work on Stu2p, eight different classes of MAPs have now been shown to interact with SUMO. These are tau (Dorval and Fraser, 2006), Ndc80p (Montpetit et al., 2006), CENP-E (Zhang et al., 2008), Kar9p and Bim1p/EB1 (Leisner et al., 2008; Meednu et al., 2008), as well as Pac1p/Lis1 and Bik1p/CLIP-170 (Alonso et al., 2012). Interestingly, Stu2p interacts with five of these. Future work will elucidate the extent to which SUMO modulates these interactions, either directly or indirectly.

Future work is also needed to elucidate the function of the interaction of Stu2p with SUMO. Stu2p is a multifunctional protein. In addition to its role in microtubule polymerization and nucleation, it is responsible for microtubule anchorage at MTOCs (Podolski et al., 2014; Usui, Maekawa, Pereira, & Schiebel, 2003; Wang & Huffaker, 1997). Stu2p also functions at the kinetochore, helping to attach MTs to the outer kinetochore plaque (Haase et al., 2018; Miller et al., 2016; Pearson, Maddox, Zarzar, Salmon, & Bloom, 2003; Suzuki et al., 2016). The kinetochore contains several sumoylated proteins, including its sumoylated partner, Ndc80p (Aravamudhan et al., 2014; Montpetit et al., 2006). Stu2p also functions in spindle positioning, interacting with Kar9p, Bim1p/EB1, Bik1p/CLIP-170 and Pac1p/Lis1. While there are myriad potential functions of Stu2p that SUMO could possibly influence, future work will be necessary to precisely define this role in yeast and higher organisms.

3.1 | Tubulin interactions with SUMO

Tubulin dimers are a major binding partner of Stu2p. Here, we report three lines of evidence suggesting that tubulin interacts with SUMO. Biochemically, tubulin bound to the SUMO-GA column independently of Stu2p. Beta-tubulin also interacted with SUMO by two-hybrid analysis. Both alpha- and beta-tubulin also interacted with two enzymes associated with the SUMO pathway, the E3 enzyme Nfi1p that regulates SUMO conjugation and the STUbL enzyme Ris1p. Work from previous proteomics screens has suggested that tubulin can be conjugated by SUMO (Hendriks et al., 2017). A previous BiFC bi-fluorescence screen also suggested a covalent interaction (Sung et al., 2013). Combined with our work, this suggests that tubulin can interact with SUMO by both covalent and non-covalent mechanisms.

In the two-hybrid analyses, the alpha- and beta-tubulins displayed different interactions with SUMO. Beta-tubulin interacted with SUMO, whereas the two alpha-tubulins did not. Notably, the beta-tubulin interaction with SUMO was retained under benomyl treatment, as was the Tub2p-Ris1p interaction. In contrast, benomyl eliminated all of the interactions of the alpha-tubulins that we analyzed (Tub2p, the E3 Nfi1, the STUbL Ris1p, and neck protein Nis1p). These findings are consistent with a model in which the alpha-tubulin interactions with SUMO are bridged or facilitated by beta-tubulin.

Our observations that SUMO and the STUbL Ris1p interact preferentially with beta-tubulin are especially relevant in light of the well-documented fact that excess beta-tubulin is toxic to the cell (Burke, Gasdaska, & Hartwell, 1989; Katz, Weinstein, & Solomon, 1990; Weinstein & Solomon, 1990). Previous work has demonstrated that cells maintain the 1:1 stoichiometry between alpha- and beta-tubulin using a variety of mechanisms, including co-translational regulation of beta-tubulin mRNA degradation and beta-tubulin binding proteins or chaperones (Abruzzi, Smith, Chen, & Solomon, 2002; Theodorakis & Cleveland, 1992). We speculate that excess beta-tubulin could be degraded through STUbL pathways. This would represent a novel mechanism by which tubulin homeostasis could be regulated by the cell.

4 | MATERIALS AND METHODS

4.1 | Two-hybrid analysis

Two-hybrid analysis was carried out as previously described (Meednu et al., 2008; Moore & Miller, 2007; Moore et al., 2008). All analysis was carried out after 2–3 days of growth at 30°C. *STU2*-BD (pRM7247/pCUB495) was a gift from Tim Huffaker.

4.2 | *GAL4*-BD m*TUB2* construction

Mutant Tub2 was PCR amplified from AD-mTub2 (pRM2117) using primers #1196 5′-ATTAGACTACCCGGGATGAGAGAAATCATTCA TATCTCG-3′ and #1197 5′-CGCTTATAACTGCAGTTATTCAAAATTCT CAGTGATT-3.' The PCR product was cloned into XmaI and PstI sites of pGBD-C1 vector (pRM1157). This created the Gal4 DBD-mTub2 yeast two-hybrid construct (pRM10749).

4.3 | His_6-SUMO-GG construction

SMT3 sequence was amplified from pRM4920 using primer #568 5′-CGGGATCCATGTCGGACTCAGAAGTC-3′ and #570 5′-CGCTCGAGC TAACCACCAATCTGTTCTCTG-3′. This generated a SUMO lacking the three terminal amino acids, ATY. A stop codon was added immediately following the glycine 98 residue to generate SUMO in the activated form. The PCR product was cloned into pET-30a(+) (pRM634) at BamHI and XhoI restriction sites. The resulting plasmid was sequenced for verification, generating pRM6711. To express His_6-Smt3p-GG, the plasmid was transformed into BL21-Gold(DE3) (Agilent Technologies, Santa Clara, CA) bacteria, and stored as pRM6713.

4.4 | His_6-SUMO-GA construction

Primers #568 5′-CGGGATCCATGTCGGACTCAGAAGTC-3′ and #571 5′-CGCTCGAGCTAAGCACCAATCTGTTCTCTG-3′ were used to amplify *SMT3* sequence from pRM4920. Primer #571 incorporated mutations that change glycine98 to alanine and a stop codon that follows the mutated alanine residue. The PCR product was cloned into the BamHI and XhoI restriction sites of pET-30(+) (pRM634) to create pRM6720. The accuracy of the construct was confirmed by sequencing. The plasmid was transformed into BL21-Gold(D3) cells, generating pRM6721.

4.5 | GST-SUMO-GA construction

SUMO-GA was PCR amplified using pRM9157 template DNA and primers #854 5'CAACTAATCGTCGACTATGTCGGACTCAGAAGTC-3′ and #328 5′-CGTGGAGCTCCCTAATACGTAGCACCACC-3′. SUMO-GA was cloned into the SalI and SacI sites of modified pGEXT-4T-2 vector (pRM2759) in which the NotI site had been replaced with a linker containing the SacI restriction site. This created the GST-SUMO-GA fusion (pRM10097).

4.6 | SUMO-GST construction

To engineer a SUMO-GST fusion construct (pRM10815), GST was PCR amplified from pGEX-4T-2 using primers #1191 5′-TTATCGCATG GGCCCGTATTCATGTCCCCTATAC-3′ and #1192 5′-GTTCGAGTAGGG CCCCTATTGAACCAGATCCGATTTTG-3′ and cloned into the ApaI site of pRS415 to generate pRM10655.

SMT3-GG was then PCR amplified from *S. cerevisiae* genomic DNA using primers #1186 5′-TTATCGCATGGATCCCGATGTCGGACTCA GAAG-3′ and #1187 5′-ATAGACACGACTCGTCTCGAGACCACCAAT CTGTTCTCTG-3′ and ligated into BamHI and XhoI sites upstream of GST in pRM10655 to make pRM10657.

SMT3-GST containing a serine 2 to alanine mutation was PCR amplified from pRM10657 using primers #1233 5′-GATGTACGAC CATG GCGGACTCAGAAGTC-3′ and #1234 5′-TATCAGCTAGGATCCC TATTT TGGAGGATGGTC-3′ and ligated into the NcoI and BamHI restriction sites of pET21d(+) to generate pRM10763. Lastly, the S2A mutation was reverted to the wild-type alanine by site-directed mutagenesis using primers #1240 5′-CTTTAAGAAGGAGATATACCATGTCG GACTCA GAAGTCAATCAAG-3′ and #1241 5′-CTTGATTGACTTCTGA GTCCGAC ATGGTATATCTCCTTCTTAAAG-3′ to make pRM10818. SUMO-GST was expressed and purified from BL21-Gold(DE3) bacteria (Agilent Technologies, Santa Clara, CA).

4.7 | *In vitro* sumoylation assay

Stu2p was sumoylated using a protocol described previously (Alonso et al., 2012; Meednu et al., 2008).

4.8 | Purification of his_6-SUMO-GG, his_6-SUMO-GA, and his_6-Ubc9p

To express and purify his_6-Smt3p-GG (pRM6713), his_6-Smt3-GA (pRM6721), and his_6-Ubc9p (pRM5169), bacteria containing each plasmid were grown overnight in LB plus 50 mg/mL Kanamycin. Saturated cultures were diluted 1:50 into 500 mL of fresh LB plus 50 mg/mL Kanamycin and grown at 37 °C for approximately 2 h to obtain the OD600 between 0.7-0.8. To induce protein expression, 1 mM IPTG was added to the culture and were grown an additional 2 h at 37 °C. Cells were harvested by centrifugation at 4,000 rpm. Extracts was prepared by resuspending the cells in 1x binding buffer (20 mM Tris pH 7.9, 300 mM NaCl, 5 mM imidazole) supplemented with bacterial protease inhibitor (Sigma Chemical, St. Louis, MO) and 1mM PMSF before lysing cells by sonication. Extracts were clarified by centrifugation at 13,000 rpm for 30 min at 4 °C. The supernatant was collected and protein concentration was determined by the Bradford assay using BSA as a standard.

Nickel-NTA resin was used to enrich six histidine-tagged proteins (Novagen, Inc. Madison, WI). Resins were charged according to the manufacturer protocol. Extracts were applied to 2 mL of slurry of the charged nickel resin. Protein was allowed to bind for 30 min on a rotisserie at 4 °C. The resin was collected by centrifugation at 1,000 rpm for 1 min and the unbound protein was discarded. The resin was then washed as follows: 10 mL of 1× binding buffer with 5 mM imidazole, 10 mL of 1× binding buffer with 50 mM imidazole, and 10 mL of 1× binding buffer with 100 mM imidazole. During each wash, resin was allowed to incubate with the buffer for 10 min on a rotisserie at 4 °C and collected by centrifugation at 1000 rpm after each wash. To elute bound protein, 1 mL of 1× binding buffer containing 400 mM imidazole was added to the resin and incubated for 10 min at 4 °C. The eluent was collected by centrifugation at 1,000 rpm for 1 min. The supernatant was transferred to a fresh tube and the resin was discarded. The protein was aliquoted, flash frozen with liquid nitrogen, and stored at −80 °C for future use.

For the *in vitro* sumoylation assay, protein was dialyzed with the sumoylation assay buffer (50 mM Tris pH 7.6, 5 mM $MgCl_2$, 15% glycerol) overnight at 4 °C. The concentration of the protein after dialysis was determined by the Bradford assay (BIO-Rad, Hercules, CA). After dialysis, Coomassie-blue staining of SDS-PAGE and western blotting using anti-his6 were used to determine the purity of the purified protein.

4.9 | Purification of GST-Aos1p and Uba2p

GST-Aos1p and Uba2p (pRM6730) were purified as described (Bencsath, Podgorski, Pagala, Slaughter, & Schulman, 2002; Meednu et al., 2008). The two proteins were coexpressed from a bi-cistronic vector and co-purified from bacteria using glutathione affinity chromatography. The bacteria were grown overnight to obtain a saturated culture in LB plus 50 mg mL^{-1} ampicillin. Saturated cultures were diluted 1:50 into 500 mL fresh LB plus 50 mg mL^{-1} ampicillin. The culture was grown to the OD 0.7-0.8 at 37 °C. To induce expression of the protein, 1 mM IPTG was added and the culture was grown at 37 °C for an additional 2 h. Cells were collected by centrifugation at 4,000 rpm and washed once with PBS. Cell pellets were resuspended in PBS containing 1% Triton-X 100, bacteria protease inhibitor, and 1 mM PMSF.

Cells were lysed by sonication and centrifuged at 13,000 rpm for 30 min to clarify the protein extract.

Glutathione affinity chromatography was used to purify GST-Aos1p/Uba2p. A 1.5 mL slurry of glutathione beads (Amersham Biosciences, Piscataway, NJ) was equilibrated with PBS. Clarified extracts were applied to the equilibrated glutathione beads and allowed to bind for 1 h at 4 °C on a rotisserie. The beads were collected by centrifugation at 1,000 rpm for 1 min and the unbound fraction was discarded. The beads were then washed three times with 10 mL of PBS. Each time, the beads were mixed with the buffer for 10 min on a rotisserie at 4 °C and collected by centrifugation. To elute the protein from the beads, the fusion protein was cleaved with thrombin overnight on ice. The protein was then dialyzed into the sumoylation assay buffer (50 mM Tris, pH 7.6, 5 mM $MgCl_2$, 15% glycerol). The concentration of protein after dialysis was determined by Bradford assay. Protein purity was evaluated with an anti-GST western blot and Coomassie-blue stained SDS-PAGE. The protein was aliquoted, flash frozen with liquid nitrogen, and stored at −80 °C for subsequent use.

4.10 | Stu2p-TAP purification

TAP-tagged Stu2p was expressed under the *GAL1* inducible promoter (Gelperin et al., 2005). A wild-type yeast strain (yRM7230) containing pGAL-*STU2*-TAP was grown to mid-exponential phase in SC -ura media containing 2% sucrose and induced with 2% galactose for 4 h at 30 °C. Cell lysates were prepared by breaking open the cell with glass beads in 1x binding buffer supplemented with yeast protease inhibitor cocktail and 1 mM PMSF. After clarification, lysates were applied to charged nickel resin (Novagen, Madison, WI) and incubated for 1.5 hr at 4 °C. The beads were first washed with 35 mL 1x binding buffer, followed by washing with 1x binding buffer plus 50 mM imidazole. To elute the bound protein, resin was incubated with 5 mL of 1x binding buffer supplemented with 400 mM imidazole, and 1.5 mL fractions were collected. The fractions were then dialyzed in sumoylation assay buffer (50 mM Tris pH 7.6, 5 mM $MgCl_2$, 15% glycerol) overnight at 4 °C.

4.11 | *In vitro* sumoylation of Stu2-TAP

To perform the *in vitro* sumoylation assay, one microgram of purified Stu2p-TAP was incubated with 5 μg of His6-Smt3p-GG, His6-Ubc9p, 2 μg Aos1/Uba2p, 4 mM ATP and 7 μL of an ATP regeneration system (3.5 U mL^{-1} creatine kinase, 10 mM creatine phosphate and 0.6 U mL^{-1} inorganic pyrophosphatase (Sigma Chemical Company, St. Louis, MO)). The mixture was incubated for 2 hr at 30 °C. To stop the reaction, 3x Laemmli sample buffer plus 5% beta-mercaptoethanol was added and samples were boiled for 5 min. Reaction products were subjected to 6% SDS-PAGE and visualized by western blot analysis. The presence of Stu2p-TAP was confirmed using mouse anti-HA (Santa Cruz Biotechnology, CA).

4.12 | Preparation of whole-cell extracts

Ulp1-ts strains expressing Stu2-HA (pRM2119) or vector (pRM2200) were grown to saturation in SC –Leu –Trp liquid media. Cells were collected by low speed centrifugation, washed, and resuspended in cold 1x PBS containing 0.1% Tween buffer and excess fluid was removed. Cells were resuspended in 1× PBS containing 0.1% Tween, 1 mM PMSF, 20 mM N-ethylmaleimide, 40 mM 2-iodoacetamide, and 1% Sigma protease inhibitor cocktail. Cells were lysed by vortexing with glass beads for 10 min. Extracts were clarified by centrifugation at 13,500*g* for 20 min at 4 °C. Protein concentrations were determined by Bradford Protein Assay (Bio-Rad, Hercules, CA), using BSA as a standard. Protein samples were analyzed by 10% SDS-PAGE followed by western blotting.

4.13 | Stu2p pull-down assay

Yeast whole-cell extracts were prepared as described above by bead beating. Extracts were incubated with agarose anti-HA beads (cat# A2095, Sigma Aldrich, St. Louis, MO,) at 4 °C on a rotisserie for 2 hr. Beads were collected and washed twice with ice-cold PBS containing an additional 0.5 M NaCl, for a total of 650 mM NaCl. To elute, beads were boiled with 3x Laemmli sample buffer for 5 min. Stu2-HA was detected using rabbit anti-HA antibody (Sigma Aldrich, St. Louis, MO, Cat #H6908) at 1:1500 in PBS for 2 hr at RT. SUMO was detected using rabbit anti-Smt3p (Rockland, Inc. Gilbertsville, PA, Cat #200–401-428) at 1:1000 in PBS for 2 hr at RT.

4.14 | Stu2-his6 enrichment under denaturing conditions

To prepare yeast whole-cell extracts, strains expressing Stu2-his6 (yRM9417) or non-tagged Stu2p (yRM2146) were grown overnight to saturation. Cells were resuspended in PBS buffer containing a 2x protease inhibitor cocktail (2 mM PMSF, 86 mM 2-Iodoacetamide, 40 mM NEM, and 1:250 Sigma PIC-P8849) at a ratio of 1 mL of buffer to every 3 g of cell pellet by weight. The cell suspension was flash frozen by pipetting droplets into liquid nitrogen and stored at −80 °C. Cells were re-chilled in liquid nitrogen and mechanically fractured using a Retsch MM400 cryomill. Frozen-powdered extract was resuspended to a final concentration of 3.2 mg mL^{-1} and 8 M urea in PBS containing 1× protease inhibitor cocktail lacking divalent metal ion chelators (Sigma). To clarify, extracts were centrifuged for 30 min at 16,000 RPM at 4 °C. Ni-NTA agarose resin (100 μL) that was equilibrated in 8M urea/PBS was incubated with ∼100 mg of clarified extracts for 2.5 hr at 4 °C. Resin was washed five times with 1 mL ice-cold PBS containing 8 M urea. Excess buffer from the final wash was removed using a gel-loading tip. To elute, resin was boiled with 150 μL of 2x Laemmli sample buffer. Proteins were resolved on 10% SDS-PAGE and transferred to nitrocellulose membranes. Following overnight blocking with 0.1% I-block reagent (Applied Biosystems, Bedford, MA) dissolved in PBS containing 0.1% Tween. Proteins were detected with rabbit anti-Stu2p or goat anti-SUMO (SC-11847) and goat anti-rabbit (SC-2004) or donkey anti-goat (SC-2056) conjugated with HRP.

4.15 | SUMO pull-down assay

Yeast extracts were prepared as described above. Extracts were incubated overnight with rabbit anti-Smt3p (Rockland, Gilbertsville, PA Cat

#200–401-428). Beads were collected and washed twice with cold PBS containing an additional 0.5 M NaCl, for a total of 637 mM NaCl. To elute, beads were boiled with 3x Laemmli sample buffer for 5 min. Stu2-HA was detected using mouse anti-HA antibody (Sigma Aldrich, St. Louis, MO, #3663) at 1:1500 in PBS for 2 hr at RT.

4.16 | Ubiquitin pull-down assay

Yeast extracts were prepared as described above. Extracts were incubated overnight with rabbit anti-ubiquitin (Enzo Life Sciences, Inc. Farmingdale, NY Cat #BML-UG9511-0025). Beads were collected and washed twice with ice cold PBS containing an additional 0.5 M NaCl, for a total of 637 mM NaCl. Beads were boiled with 3x sample buffer for 5 min. Stu2p was detected using mouse anti-HA (Sigma Aldrich, St. Louis, MO, Cat #H3663) at 1:1500 dilution in PBS for 2 hr at RT.

4.17 | Noncovalent binding to SUMO affinity columns

Noncovalent SUMO affinity columns were prepared as follows. Glutathione agarose beads (Pierce, Rockford, IL) were equilibrated in PBS containing 0.1% Triton, 1 mM PMSF. Bacterial cells expressing GST, GST-SUMO-GA, or SUMO-GST were disrupted by sonication in PBS buffer containing 0.1% Triton, 1 mM PMSF. To clarify, extracts were centrifuged at 13,000 RPM for 30 min at 4 °C. Bacterial extracts were incubated with 100 μL of glutathione agarose beads for 2 hr with gentle agitation. Resins were then washed two times with 150 column volumes of PBS containing 0.1% Triton. Aliquots of the GST or SUMO-GST affinity matrices were run on SDS-PAGE in triplicate, stained with coomassie blue, analyzed by densitometry, and normalized for subsequent affinity assays. It is interesting to note that for Nis1p, little or no binding was observed when the Nis1p protein was applied to the columns at concentrations higher than 2 mg mL^{-1}. This may indicate that complexes can mask the SUMO interaction motif in Nis1p (data not shown).

To prepare yeast whole-cell extracts, cells expressing Stu2–3xHA (pRM10637) or Nis1p-6xHA (pRM10782) from CEN plasmids were grown overnight to saturation. Cells were disrupted by bead beating or by cryomilling in liquid nitrogen in PBS containing 0.1% Triton, 1 mM PMSF, 43 mM 2-Iodoacetamide, 20 mM NEM, and 1:500 dilution of Sigma Protease Inhibitor Cocktail P8215 developed for *S. cerevisiae*. The indicated amounts of extracts containing Nis1p-6xHA (2 mgs), Stu2–3xHA (10.8mgs), or the empty vector control (10.8mgs) were incubated with normalized amounts of GST, GST-SUMO-GA, and SUMO-GST on a rotisserie for 3.5 h. Beads were then collected by low-speed centrifugation at 250 RPM for 1 min and washed 5 times with 1 mL PBS. The final wash was removed completely using a gel-loading tip. To elute bound protein, beads were resuspended in 70 μL 2x-Laemmli sample buffer and boiled for 5 min. To confirm the column normalizations, 5% of each pull down was assayed on Coomassie blue stained SDS-PAGE gels. To visualize HA epitope-tagged proteins, pull-downs were immunoblotted with mouse anti-HA (SC-7392, Santa Cruz Biotechnology, Santa Cruz, CA) and goat anti-mouse-HRP (Santa Cruz Biotechnology, Santa Cruz, CA) secondary antibody. Western blots were stripped and re-probed with anti-alpha-tubulin (YOL1/34 from AbD Serotec, Raleigh, N.D.).

ACKNOWLEGMENTS

The authors thank the reviewers for their helpful comments. This work was supported by grants from the Oklahoma Health Research Program of the Oklahoma Center for the Advancement of Science and Technology (OCAST #HR09–150S), NSF (#MCB-0414768 and #MCB-1052174), NIH (R15GM119117-01) and the Oklahoma Agricultural Experiment Station (OKL02961) to RKM. AA was supported in part by a fellowship from the Sloan Foundation. RC and KD were supported in part by the NSF-funded Louis Stokes Alliance for Minority Participation (OK-LSAMP) program at OSU.

REFERENCES

Abruzzi, K. C., Smith, A., Chen, W., & Solomon, F. (2002). Protection from free beta-tubulin by the beta-tubulin binding protein Rbl2p. *Molecular Cell Biology*, *22*(1), 138–147.

Al-Bassam, J., & Chang, F. (2011). Regulation of microtubule dynamics by TOG-domain proteins XMAP215/Dis1 and CLASP. *Trends in Cell Biology*, *21*(10), 604–614.

Al-Bassam, J., Larsen, N. A., Hyman, A. A., & Harrison, S. C. (2007). Crystal structure of a TOG domain: Conserved features of XMAP215/Dis1-family TOG domains and implications for tubulin binding. *Structure*, *15*(3), 355–362.

Al-Bassam, J., van Breugel, M., Harrison, S. C., & Hyman, A. A. (2006). Stu2p binds tubulin and undergoes an open-to-closed conformational change. *The Journal of Cell Biology*, *172*(7), 1009–1022.

Alonso, A., D'Silva, S., Rahman, M., Meluh, P. B., Keeling, J., Meednu, N., … Miller, R. K. (2012). The yeast homologue of the microtubule-associated protein Lis1 interacts with the sumoylation machinery and a SUMO-targeted ubiquitin ligase. *Molecular Biology of the Cell*, *23*(23), 4552–4566.

Alonso, A., Greenlee, M., Matts, J., Kline, J., Davis, K. J., & Miller, R. K. (2015). Emerging roles of sumoylation in the regulation of actin, microtubules, intermediate filaments, and septins. *Cytoskeleton (Hoboken, N.J.)*, *72*(7), 305–339.

Aravamudhan, P., Felzer-Kim, I., Gurunathan, K., & Joglekar, A. P. (2014). Assembling the protein architecture of the budding yeast kinetochore-microtubule attachment using FRET. *Current Biology*, *24*(13), 1437–1446.

Ayaz, P., Ye, X., Huddleston, P., Brautigam, C. A., & Rice, L. M. (2012). A TOG: Alpha-beta tubulin complex structure reveals conformational-based mechanisms for a microtubule polymerase. *Science*, *337*(6096), 857–860.

Bencsath, K. P., Podgorski, M. S., Pagala, V. R., Slaughter, C. A., & Schulman, B. A. (2002). Identification of a multifunctional binding site on Ubc9p required for Smt3p conjugation. *The Journal of Biological Chemistry*, *277*(49), 47938–47945.

Blake-Hodek, K. A., Cassimeris, L., & Huffaker, T. C. (2010). Regulation of microtubule dynamics by Bim1 and Bik1, the budding yeast members of the EB1 and CLIP-170 families of plus-end tracking proteins. *Molecular Biology of the Cell*, *21*(12), 2013–2023.

Bloom, K. (2000). It's a kar9ochore to capture microtubules. *Nature Cell Biology*, *2*(6), E96–E98.

Bossis, G., Malnou, C. E., Farras, R., Andermarcher, E., Hipskind, R., Rodriguez, M., … Piechaczyk, M. (2005). Down-regulation of c-Fos/c-Jun

AP-1 dimer activity by sumoylation. *Molecular Cell Biology*, *25*(16), 6964–6979.

Brouhard, G. J., Stear, J. H., Noetzel, T. L., Al-Bassam, J., Kinoshita, K., Harrison, S. C., … Hyman, A. A. (2008). XMAP215 is a processive microtubule polymerase. *Cell*, *132*(1), 79–88.

Burke, D., Gasdaska, P., & Hartwell, L. (1989). Dominant effects of tubulin overexpression in *Saccharomyces cerevisiae*. *Molecular and Cellular Biology*, *9*(3), 1049–1059.

Bylebyl, G. R., Belichenko, I., & Johnson, E. S. (2003). The SUMO isopeptidase Ulp2 prevents accumulation of SUMO chains in yeast. *Journal of Biological Chemistry*, *278*(45), 44113–44120.

Coquelle, F. M., Caspi, M., Cordelieres, F. P., Dompierre, J. P., Dujardin, D. L., Koifman, C., … Galjart, N. (2002). LIS1, CLIP-170's key to the dynein/dynactin pathway. *Molecular and Cellular Biology*, *22*(9), 3089–3102.

Dorval, V., & Fraser, P. E. (2006). Small ubiquitin-like modifier (SUMO) modification of natively unfolded proteins tau and alpha-synuclein. *Journal of Biological Chemistry*, *281*(15), 9919–9924.

Elmore, Z. C., Donaher, M., Matson, B. C., Murphy, H., Westerbeck, J. W., & Kerscher, O. (2011). SUMO-dependent substrate targeting of the SUMO protease Ulp1. *BMC Biology*, *9*(1), 74.

Gareau, J. R., & Lima, C. D. (2010). The SUMO pathway: emerging mechanisms that shape specificity, conjugation and recognition. *Nature Reviews Molecular Cell Biology*, *11*(12), 861–871.

Gelperin, D. M., White, M. A., Wilkinson, M. L., Kon, Y., Kung, L. A., Wise, K. J., … Yu, H. (2005). Biochemical and genetic analysis of the yeast proteome with a movable ORF collection. *Genes & Development*, *19*(23), 2816–2826.

Gundersen, G. G., & Bretscher, A. (2003). Microtubule asymmetry. *Science (New York, N.Y.)*, *300*(5628), 2040.

Haase, K. P., Fox, J. C., Byrnes, A. E., Adikes, R. C., Speed, S. K., Haase, J., … Rusan, N. M. (2018). Stu2 uses a 15 nm parallel coiled coil for kinetochore localization and concomitant regulation of the mitotic spindle. *Molecular Biology of the Cell*, *29*(3), 285–294.

Hecker, C. M., Rabiller, M., Haglund, K., Bayer, P., & Dikic, I. (2006). Specification of SUMO1- and SUMO2-interacting motifs. *The Journal of Biological Chemistry*, *281*(23), 16117–16127.

Hendriks, I. A., Lyon, D., Young, C., Jensen, L. J., Vertegaal, A. C., & Nielsen, M. L. (2017). Site-specific mapping of the human SUMO proteome reveals co-modification with phosphorylation. *Nature Structural & Molecular Biology*, *24*(3), 325–336.

Humphrey, L., Felzer-Kim, I., & Joglekar, A. P. (2018). Stu2 acts as a microtubule destabilizer in metaphase budding yeast spindles. *Molecular Biology of the Cell*, *29*(3), 247–255.

James, P., Halladay, J., & Craig, E. A. (1996). Genomic libraries and a host strain designed for highly efficient two-hybrid selection in yeast. *Genetics*, *144*, 1425–1436.

Jardin, C., Horn, A. H., & Sticht, H. (2015). Binding properties of SUMO-interacting motifs (SIMs) in yeast. *Journal of Molecular Modeling*, *21*(3), 50.

Johnson, E. S., & Blobel, G. (1997). Ubc9p is the conjugating enzyme for the ubiquitin-like protein Smt3p. *The Journal of Biological Chemistry*, *272*(43), 26799–26802.

Johnson, E. S., & Gupta, A. A. (2001). An E3-like factor that promotes SUMO conjugation to the yeast septins. *Cell*, *106*(6), 735–744.

Katz, W., Weinstein, B., & Solomon, F. (1990). Regulation of tubulin levels and microtubule assembly in *Saccharomyces cerevisiae*: Consequences of altered tubulin gene copy number. *Molecular and Cellular Biology*, *10*(10), 5286–5294.

Kerscher, O., Felberbaum, R., & Hochstrasser, M. (2006). Modification of proteins by ubiquitin and ubiquitin-like proteins. *Annual Review of Cell and Developmental Biology*, *22*, 159–180.

Kitamura, E., Tanaka, K., Komoto, S., Kitamura, Y., Antony, C., & Tanaka, T. U. (2010). Kinetochores generate microtubules with distal plus ends: Their roles and limited lifetime in mitosis. *Developmental Cell*, *18*(2), 248–259.

Kosco, K. A., Pearson, C. G., Maddox, P. S., Wang, P. J., Adams, I. R., Salmon, E. D., … Huffaker, T. C. (2001). Control of microtubule dynamics by Stu2p is essential for spindle orientation and metaphase chromosome alignment in yeast. *Molecular Biology of the Cell*, *12*(9), 2870–2880.

Kroetz, M. B., & Hochstrasser, M. (2009). Identification of SUMO-interacting proteins by yeast two-hybrid analysis. *Methods of Molecular Biology*, *497*, 107–120.

Lee, L., Tirnauer, J. S., Li, J., Schuyler, S. C., Liu, J. Y., & Pellman, D. (2000). Positioning of the mitotic spindle by a cortical-microtubule capture mechanism. *Science*, *287*(5461), 2260–2262.

Leisner, C., Kammerer, D., Denoth, A., Britschi, M., Barral, Y., & Liakopoulos, D. (2008). Regulation of mitotic spindle asymmetry by SUMO and the spindle-assembly checkpoint in yeast. *Current Biology*, *18*(16), 1249–1255.

Li, S.-J., & Hochstrasser, M. (1999). A new protease required for cell-cycle progression in yeast. *Nature*, *398*(6724), 246–251.

Li, S. J., & Hochstrasser, M. (2000). The yeast *ULP2(SMT4)* gene encodes a novel protease specific for the ubiquitin-like Smt3 protein. *Molecular and Cellular Biology*, *20*(7), 2367–2377.

Liakopoulos, D., Kusch, J., Grava, S., Vogel, J., & Barral, Y. (2003). Asymmetric loading of Kar9 onto spindle poles and microtubules ensures proper spindle alignment. *Cell*, *112*(4), 561–574.

Ma, L., McQueen, J., Cuschieri, L., Vogel, J., & Measday, V. (2007). Spc24 and Stu2 promote spindle integrity when DNA replication is stalled. *Molecular Biology of the Cell*, *18*(8), 2805–2816.

Markus, S. M., Plevock, K. M., St. Germain, B. J., Punch, J. J., Meaden, C. W., & Lee, W. L. (2011). Quantitative analysis of Pac1/Lis1-mediated dynein targeting: Implications for regulation of dynein activity in budding yeast. *Cytoskeleton*, *68*(3), 157–174.

Meednu, N., Hoops, H., D'Silva, S., Pogorzala, L., Wood, S., Farkas, D., … Miller, R. K. (2008). The spindle positioning protein Kar9p interacts with the sumoylation machinery in *Saccharomyces cerevisiae*. *Genetics*, *180*(4), 2033–2055.

Miller, M. P., Asbury, C. L., & Biggins, S. (2016). A TOG protein confers tension sensitivity to kinetochore-microtubule attachments. *Cell*, *165*(6), 1428–1439.

Miller, R. K., Cheng, S.-C., & Rose, M. D. (2000). Bim1p/Yeb1p mediates the Kar9p-dependent cortical attachment of cytoplasmic microtubules. *Molecular Biology of the Cell*, *11*(9), 2949–2959.

Miller, R. K., Matheos, D., & Rose, M. D. (1999). The cortical localization of the microtubule orientation protein, Kar9p, is dependent upon actin and proteins required for polarization. *The Journal of Cell Biology*, *144*(5), 963–975.

Miller, R. K., & Rose, M. D. (1998). Kar9p is a novel cortical protein required for cytoplasmic microtubule orientation in yeast. *The Journal of Cell Biology*, *140*(2), 377–390.

Montpetit, B., Hazbun, T. R., Fields, S., & Hieter, P. (2006). Sumoylation of the budding yeast kinetochore protein Ndc10 is required for Ndc10 spindle localization and regulation of anaphase spindle elongation. *The Journal of Cell Biology*, *174*(5), 653–663.

Moore, J. K., D'Silva, S., & Miller, R. K. (2006). The CLIP-170 homologue Bik1p promotes the phosphorylation and asymmetric localization of Kar9p. *Molecular Biology of the Cell*, *17*(1), 178–191.

Moore, J. K., Li, J., & Cooper, J. A. (2008). Dynactin function in mitotic spindle positioning. *Traffic (Copenhagen, Denmark)*, *9*(4), 510–527.

Moore, J. K., & Miller, R. K. (2007). The cyclin-dependent kinase Cdc28p regulates multiple aspects of Kar9p function in yeast. *Molecular Biology of the Cell*, *18*(4), 1187–1202.

Mullen, J. R., Chen, C.-F., & Brill, S. J. (2010). Wss1 is a SUMO-dependent isopeptidase that interacts genetically with the Slx5-Slx8 SUMO-targeted Ub ligase. *Molecular Cell Biology*, *30*(15), 3737–3748.

Newman, H. A., Meluh, P. B., Lu, J., Vidal, J., Carson, C., Lagesse, E., … Matunis, M. J. (2017). A high throughput mutagenic analysis of yeast sumo structure and function. *PLoS Genetics*, *13*(2), e1006612.

Okada, N., Toda, T., Yamamoto, M., & Sato, M. (2014). CDK-dependent phosphorylation of Alp7-Alp14 (TACC-TOG) promotes its nuclear accumulation and spindle microtubule assembly. *Molecular Biology of the Cell*, *25*(13), 1969–1982.

Park, C. J., Park, J.-E., Karpova, T. S., Soung, N.-K., Yu, L.-R., Song, S., … Dabanoglu, I. (2008). Requirement for the budding yeast polo kinase Cdc5 in proper microtubule growth and dynamics. *Eukaryotic Cell*, *7*(3), 444–453.

Pearson, C. G., Maddox, P. S., Zarzar, T. R., Salmon, E. D., & Bloom, K. (2003). Yeast kinetochores do not stabilize Stu2p-dependent spindle microtubule dynamics. *Molecular Biology of the Cell*, *14*(10), 4181–4195.

Pichler, A., Fatouros, C., Lee, H., & Eisenhardt, N. (2017). SUMO conjugation—A mechanistic view. *Biomolecular Concepts*, *8*(1), 13–36.

Podolski, M., Mahamdeh, M., & Howard, J. (2014). Stu2, the budding yeast XMAP215/Dis1 homolog, promotes assembly of yeast microtubules by increasing growth rate and decreasing catastrophe frequency. *Journal of Biological Chemistry*, *289*(41), 28087–28093.

Praefcke, G. J., Hofmann, K., & Dohmen, R. J. (2012). SUMO playing tag with ubiquitin. *Trends in Biochemical Sciences*, *37*(1), 23–31.

Puig, O., Caspary, F., Rigaut, G., Rutz, B., Bouveret, E., Bragado-Nilsson, E., … Seraphin, B. (2001). The tandem affinity purification (TAP) method: A general procedure of protein complex purification. *Methods*, *24*(3), 218–229.

Rojas-Fernandez, A., Plechanovova, A., Hattersley, N., Jaffray, E., Tatham, M. H., & Hay, R. T. (2014). SUMO chain-induced dimerization activates RNF4. *Molecular Cell*, *53*(6), 880–892.

Schweiggert, J., Stevermann, L., Panigada, D., Kammerer, D., & Liakopoulos, D. (2016). Regulation of a spindle positioning factor at kinetochores by SUMO-targeted ubiquitin ligases. *Developmental Cell*, *36*(4), 415–427.

Sheeman, B., Carvalho, P., Sagot, I., Geiser, J., Kho, D., Hoyt, M. A., & Pellman, D. (2003). Determinants of *S. cerevisiae* dynein localization and activation: Implications for the mechanism of spindle positioning. *Current Biology*, *13*(5), 364–372.

Shirasu-Hiza, M., Coughlin, P., & Mitchison, T. (2003). Identification of XMAP215 as a microtubule-destabilizing factor in Xenopus egg extract by biochemical purification. *The Journal of Cell Biology*, *161*(2), 349–358.

Sikorski, R. S., & Hieter, P. (1989). A system of shuttle vectors and yeast host strains designed for efficient manipulation of DNA in *Saccharomyces cerevisiae*. *Genetics*, *122*, 19–27.

Slep, K. C., & Vale, R. D. (2007). Structural basis of microtubule plus end tracking by XMAP215, CLIP-170, and EB1. *Molecular Cell*, *27*(6), 976–991.

Song, J., Durrin, L. K., Wilkinson, T. A., Krontiris, T. G., & Chen, Y. (2004). Identification of a SUMO-binding motif that recognizes SUMO-modified proteins. *Proceedings of the National Academy of Sciences of the United States of America*, *101*(40), 14373–14378.

Su, D., & Hochstrasser, M. (2010). A WLM protein with SUMO-directed protease activity. *Molecular and Cellular Biology*, *30*(15), 3734–3736.

Sung, M. K., Lim, G., Yi, D. G., Chang, Y. J., Yang, E. B., Lee, K., & Huh, W. K. (2013). Genome-wide bimolecular fluorescence complementation analysis of SUMO interactome in yeast. *Genome Research*, *23*(4), 736–746.

Suzuki, A., Badger, B. L., Haase, J., Ohashi, T., Erickson, H. P., Salmon, E. D., & Bloom, K. (2016). How the kinetochore couples microtubule force and centromere stretch to move chromosomes. *Nature Cell Biology*, *18*(4), 382–392.

Tai, C.-Y., Dujardin, D. L., Faulkner, N. E., & Vallee, R. B. (2002). The role of dynein, dynactin, and CLIP-170 interactions in LIS1 kinetochore function. *The Journal of Cell Biology*, *156*(6), 959–968.

Takahashi, Y., Kahyo, T., Toh, E. A., Yasuda, H., & Kikuchi, Y. (2001). Yeast Ull1/Siz1 is a novel SUMO1/Smt3 ligase for septin components and functions as an adaptor between conjugating enzyme and substrates. *Journal of Biological Chemistry*, *276*(52), 48973–48977.

Theodorakis, N. G., & Cleveland, D. W. (1992). Physical evidence for cotranslational regulation of beta-tubulin mRNA degradation. *Molecular and Cellular Biology*, *12*(2), 791–799.

Trogden, K. P., & Rogers, S. L. (2015). TOG proteins are spatially regulated by Rac-GSK3beta to control interphase microtubule dynamics. *PLoS One*, *10*(9), e0138966.

Usui, T., Maekawa, H., Pereira, G., & Schiebel, E. (2003). The XMAP215 homologue Stu2 at yeast spindle pole bodies regulates microtubule dynamics and anchorage. *Embo Journal*, *22*(18), 4779–4793.

Uzunova, K., Gottsche, K., Miteva, M., Weisshaar, S. R., Glanemann, C., Schnellhardt, M., … Johnson, E. S. (2007). Ubiquitin-dependent proteolytic control of SUMO conjugates. *Journal of Biological Chemistry*, *282*(47), 34167–34175.

van Breugel, M., Drechsel, D., & Hyman, A. (2003). Stu2p, the budding yeast member of the conserved Dis1/XMAP215 family of microtubule-associated proteins is a plus end-binding microtubule destabilizer. *The Journal of Cell Biology*, *161*(2), 359–369.

Wang, P. J., & Huffaker, T. C. (1997). Stu2p: A microtubule-binding protein that is an essential component of the yeast spindle pole body. *The Journal of Cell Biology*, *139*(5), 1271–1280.

Weinstein, B., & Solomon, F. (1990). Phenotypic consequences of tubulin overproduction in *Saccharomyces cerevisiae*: Differences between alpha-tubulin and beta-tubulin. *Molecular and Cellular Biology*, *10*(10), 5295–5304.

Widlund, P. O., Stear, J. H., Pozniakovsky, A., Zanic, M., Reber, S., Brouhard, G. J., … Howard, J. (2011). XMAP215 polymerase activity is built by combining multiple tubulin-binding TOG domains and a basic lattice-binding region. *Proceedings of the National Academy of Sciences of the United States of America*, *108*(7), 2741–2746.

Wieczorek, M., Bechstedt, S., Chaaban, S., & Brouhard, G. J. (2015). Microtubule-associated proteins control the kinetics of microtubule nucleation. *Nature Cell Biology*, *17*(7), 907–916.

Wolyniak, M. J., Blake-Hodek, K., Kosco, K., Hwang, E., You, L., & Huffaker, T. C. (2006). The regulation of microtubule dynamics in *S. cerevisiae* by three interacting plus end tracking proteins. *Molecular Biology of the Cell*, *17*(6), 2789–2798.

Wong, J., Nakajima, Y., Westermann, S., Shang, C., Kang, J.-S., Goodner, C., … Drubin, D. (2007). A protein interaction map of the mitotic spindle. *Molecular Biology of the Cell*, *18*(10), 3800–3809.

Zhang, X.-D., Goeres, J., Zhang, H., Yen, T. J., Porter, A. C. G., & Matunis, M. J. (2008). SUMO-2/3 modification and binding regulate the association of CENP-E with kinetochores and progression through mitosis. *Molecular Cell*, *29*(6), 729–741.

Zhao, Q., Xie, Y., Zheng, Y., Jiang, S., Liu, W., Mu, W., … Ren, J. (2014). GPS-SUMO: A tool for the prediction of sumoylation sites and

SUMO-interaction motifs. *Nucleic Acids Research*, *42*(W1), W325–W330.

SUPPORTING INFORMATION

Additional Supporting Information may be found online in the supporting information tab for this article.

How to cite this article: Greenlee M, Alonso A, Rahman M, et al. The TOG protein Stu2/XMAP215 interacts covalently and noncovalently with SUMO. *Cytoskeleton*. 2018;75:290–306. https://doi.org/10.1002/cm.21449